ACS Pharmacology & Translational Science

pubs.acs.org/ptsci

Article

Tissue-Specific Proteomics Analysis of Anti-COVID-19 Nucleoside and Nucleotide Prodrug-Activating Enzymes Provides Insights into the Optimization of Prodrug Design and Pharmacotherapy Strategy

Jiapeng Li, Shuhan Liu, Jian Shi, Xinwen Wang, Yanling Xue, and Hao-Jie Zhu*

Cite This: *ACS Pharmacol. Transl. Sci.* 2021, 4, 870–887

Read Online

ACCESS | Metrics & More | Article Recommendations | Supporting Information

ABSTRACT: Nucleoside and nucleotide analogs are an essential class of antivirals for COVID-19 treatment. Several nucleoside/nucleotide analogs have shown promising effects against SARS-CoV-2 *in vitro*; however, their *in vivo* efficacy is limited. Nucleoside/nucleotide analogs are often formed as ester prodrugs to improve pharmacokinetics (PK) performance. After entering cells, the prodrugs undergo several enzymatic metabolism steps to form the active metabolite triphosphate nucleoside (TP-Nuc); prodrug activation is therefore associated with the abundance and catalytic activity of the corresponding activating enzymes. Having the activation of nucleoside/nucleotide prodrugs occur at the target site of action, such as the lung, is critical for anti-SARS-CoV-2 efficacy. Herein, we conducted an absolute quantitative proteomics study to determine the expression of relevant activating enzymes in human organs related to the PK and antiviral efficacy of nucleoside/nucleotide prodrugs, including the lung, liver, intestine, and kidney. The protein levels of prodrug-activating enzymes differed significantly among the tissues. Using catalytic activity values reported previously for individual enzymes, we calculated prodrug activation profiles in these tissues. The prodrugs evaluated in this study include nine McGuigan phosphoramidate prodrugs, two cyclic monophosphate prodrugs, two L-valyl ester prodrugs, and one octanoate prodrug. Our analysis showed that most orally administered nucleoside/nucleotide prodrugs were primarily activated in the liver, suggesting that parenteral delivery routes such as inhalation and intravenous infusion could be better options when these antiviral prodrugs are used to treat COVID-19. The results also indicated that the L-valyl ester prodrug design can plausibly improve drug bioavailability and enhance effects against SARS-CoV-2 intestinal infections. This study further revealed that an octanoate prodrug could provide a long-acting antiviral effect targeting SARS-CoV-2 infections in the lung. Finally, our molecular docking analysis suggested several prodrug forms of favipiravir and GS-441524 that are likely to exhibit favorable PK features over existing prodrug forms. In sum, this study revealed the activation mechanisms of various nucleoside/nucleotide prodrugs relevant to COVID-19 treatment in different organs and shed light on the development of more effective anti-COVID-19 prodrugs.

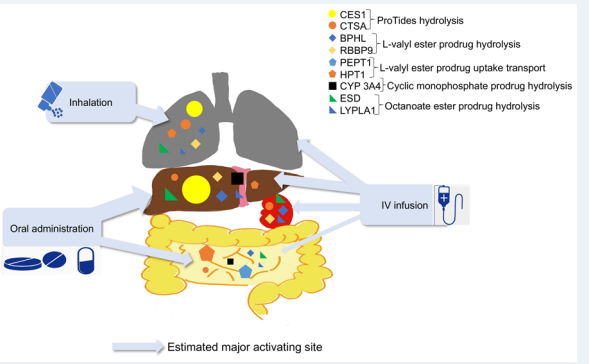

KEYWORDS: *nucleoside and nulceotide analog, SARS-CoV-2, COVID-19, prodrug, favipiravir, remdesivir, GS-441524*

Nucleoside and nucleotide analogs comprise an essential class of candidate drugs for the treatment of coronavirus disease 2019 (COVID-19), such as the nucleotide analogs remdesivir, sofosbuvir, and tenofovir alafenamide (TAF), the nucleoside analogs galidesivir and EIDD-2801, and the nucleobase analog flavipiravir.[1−4] They exert their antiviral effects via inhibiting the viral polymerase; specifically, their triphosphate metabolites (triphosphate nucleoside, TP-Nuc) mimic natural nucleosides and can be incorporated into the virus genome, upon which they terminate polymerase-mediated extension.[4] Remdesivir, an ester prodrug of the nucleoside analog GS-441524, has shown promising antiviral effects against severe acute respiratory syndrome coronavirus-2 (SARS-CoV-2) both *in vitro* and *in vivo*.[5,6] The U.S. Food and Drug Administration (FDA) recently approved remdesivir for the treatment of hospitalized COVID-19 patients. Besides remdesivir, several other nucleoside/nucleotide analogs, such as sofosbuvir and TAF, have also demonstrated some effects in suppressing SARS-CoV-2 replication *in vitro*.[4,7] Therefore, these drugs could effectively treat the infection if effective levels of the formed TP-Nuc are achieved in virally infected human cells or tissues. However, data from clinical trials has shown the *in vivo* effects of these nucleoside/nucleotide analogs to be limited in many patients.[8−10] One potential cause

Received: January 8, 2021
Published: April 1, 2021

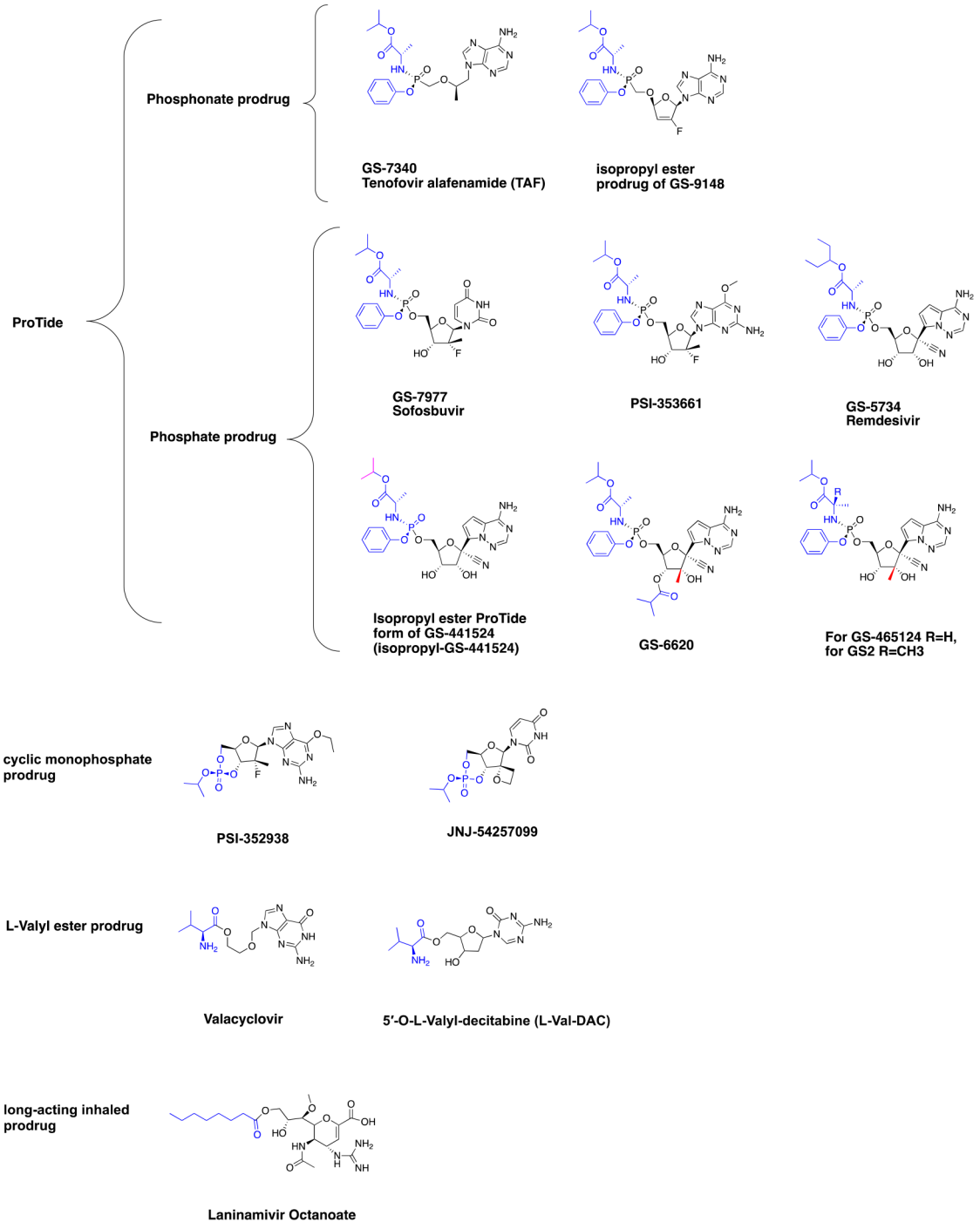

Figure 1. Molecular structures of the antiviral prodrugs evaluated in this study. The blue color highlights the ester moiety. The red color highlights the methyl group on the 2′ pentose ring in GS-6620, GS-465124, and GS2, which is the only difference in the nucleoside moiety between these compounds and remdesivir. Nine ProTides were selected, including two phosphonate prodrugs (TAF and the isopropyl ester prodrug of GS-9148) and seven phosphate prodrugs (sofosbuvir, PSI-353661, remdesivir, isopropyl-GS-441524, GS-6620, GS-465124, and GS2). Additional candidates include two cyclic monophosphate prodrugs (PSI-352938 and JNJ-54257099) two L-valyl ester prodrugs (valacyclovir and 5′-*O*-L-valyl-decitabine) and one octanoate ester prodrug (laninamivir octanoate).

for this unsatisfying outcome could be inadequate TP-Nuc concentrations at the target sites. For example, some evidence suggested that the concentration of remdesivir in lung cells may be not sufficient to treat SARS-CoV-2 infection,[11] and a combination of inhalation and intravenous (IV) administration may offer additional therapeutic benefits to patients compared to IV treatment alone.[12]

Nucleoside/nucleotide analogs are often structurally modified as ester prodrugs to improve their pharmacokinetics (PK) properties and antiviral efficacy.[13] Nucleotide analogs especially often suffer from poor cell permeability due to the natively charged phosphate or phosphonate group; their ester prodrug forms are charge-neutral and exhibit higher lipophilicity and cell permeability than the parent nucleotide forms.[14] Several prodrugs have been found to cross cell

https://doi.org/10.1021/acsptsci.1c00016
ACS Pharmacol. Transl. Sci. 2021, 4, 870−887

membranes via passive diffusion.[15,16] Once entering a cell, ester prodrugs undergo a series of enzymatic reactions to form the active metabolite TP-Nuc; these activation steps involve the initial cleavage of the ester group, the release of the nucleoside/nucleotide moiety, and the final sequential phosphorylations by native kinases.[13] Serine hydrolases have been implicated in the cleavage of the ester group of prodrugs; these enzymes constitute one of the largest and most diverse enzyme classes in humans, including more than 200 members, such as carboxylesterase 1 (CES1) and cathepsin A (CTSA).[17] The putative catalytic mechanism features the serine residual in the enzymes' serine−histidine−aspartate triad nucleophilically attacking the prodrugs' ester bond on the carboxyl side.[18] From the PK perspective, at least two factors could determine intracellular concentrations of the active metabolite TP-Nuc and its consequent antiviral efficacy: (1) the cellular load of the prodrug and (2) the intracellular activation efficiency.[14,19] Since ester prodrugs often have excellent cell permeability, the intracellular load is highly dependent on how much of the prodrug remains intact upon reaching the target cells. Importantly, after ester hydrolysis, the downstream metabolites usually carry negative charges at physiological pH, resulting in poor cell permeability and thus tend to be trapped in the cells. Thus, ester hydrolysis of prodrugs is critical for their intracellular accumulation and activation. As this hydrolytic metabolism is dependent on the catalytic activity and abundance of the corresponding activating hydrolases, it is desirable that prodrugs can be selectively activated by enzymes specifically expressed in the target site of action. When treating COVID-19 with antivirals, lung tissue is the primary site of action.[20] Unfortunately, the site of action of anti-COVID-19 prodrugs was not taken into consideration during drug development, as these antivirals were originally designed for the treatment of other indications, such as hepatitis virus and human immunodeficiency virus (HIV).

To understand and predict the intracellular activation and PK of prodrugs, tissue-specific quantitative proteomics data on the activating enzymes are essential, as protein expression levels are more closely associated with enzymatic function than are mRNA expression levels.[21−23] A recent proteomics study quantified various noncytochrome P450 (CYP) drug-metabolizing enzymes (DMEs) in assorted human tissues.[24] The expression patterns of many non-CYP DMEs differed markedly between organs, indicating tissue-dependent metabolism of non-CYP substrate drugs. However, prodrug-activating enzymes, such as serine hydrolases, have not been fully characterized in the human tissues most relevant to SARS-CoV-2 infection. In this study, we quantified the abundances of various nucleoside prodrug-activating enzymes in the human lung, liver, kidney, and intestine. We further evaluated the activation of four types of nucleoside prodrugs, including nine McGuigan phosphoramidate prodrugs (ProTides), two cyclic monophosphate prodrugs, two L-valyl ester prodrugs, and one long-acting inhaled prodrug (the chemical structures are shown in Figure 1). Moreover, we predicted their activation profiles in different tissues by collectively analyzing chemical structures, administration routes, and stability in tissue homogenates and plasma. The results shed light on the optimization of prodrug design that may lead to the development of new therapeutics with enhanced efficacy and safety for COVID-19 treatment.

METHODS

Materials. Pierce BCA protein assay kits and phosphate-buffered saline (PBS) were obtained from Thermo Fisher Scientific (Waltham, MA). All other chemicals and reagents were of analytical grade and commercially available. Pooled human lung, liver, intestine, and kidney S9 fractions were purchased from XenoTech LLC (Kansas City, KS). The donors' information is summarized in Supplementary Table 1.

Proteomics Sample Preparation. Human lung, liver, intestine, and kidney S9 samples were prepared for proteomics analysis according to a previously published method with some minor modifications.[25] Briefly, we first mixed 80 μg of S9 protein aliquot with 0.2 μg of bovine serum albumin (BSA) in a 1.5 mL microcentrifuge tube. We then added 1 mL (50-fold volume) of precooled acetone to the mixture and stored it at −20 °C overnight for protein precipitation. After this step, we centrifuged the samples at 17 000*g* for 15 min at 4 °C. The supernatant was then discarded, and the pellet was air-dried at room temperature for 5 min. We resuspended the dried pellet in 100 μL of freshly prepared 4 mM dithiolthreitol (DTT) in an 8 M urea solution containing 100 mM NH_4HCO_3. After completely dissolving the proteins via vortexing and sonication, we incubated the samples at 37 °C for 45 min for reduction and let it cool to room temperature. Next, we added 100 μL of freshly prepared 20 mM iodoacetamide (IAA) in an 8 M urea solution with 100 mM NH_4HCO_3 into the samples and incubated them at room temperature in the dark for 30 min. Subsequently, we diluted the urea concentration to 6 M by adding 56.6 μL of 50 mM NH_4HCO_3. For protein digestion, we first incubated the samples with lysyl endopeptidase (protein/lysyl endopeptidase = 100:1) in an orbital incubator shaker at 220 rpm and 37 °C for 6 h. Next, we added 733 μL of 50 mM NH_4HCO_3 to adjust the urea concentration to 1.6 M, then incubated the samples with tosyl phenylalanyl chloromethyl ketone-treated trypsin (protein/trypsin = 50:1) at 220 rpm and 37 °C overnight. We then added 1 μL of trifluoroacetic acid to terminate the digestion, extracted the digested peptides using Waters Oasis HLB columns according to the manufacturer's instructions, and dried the extracted peptides in a SpeedVac SPD1010 vacuum concentrator (Thermo Scientific, Hudson, NH). We finally resuspended the dried peptide samples in 3% acetonitrile containing 0.1% formic acid for liquid chromatography−tandem mass spectrometry (LC-MS/MS) analysis.

LC-MS/MS-Based Proteomics Analysis. The LC-MS/MS system consisted of a tandem quadrupole time-of-flight mass spectrometer (TripleTOF 5600 plus, Sciex, Framingham, MA) and an Eksigent 2D Plus LC System (Eksigent Technologies, Dublin, CA). We used a previously published data-independent analysis (DIA) method to quantify the proteins of interest.[26] Briefly, the mobile phase was composed of water with 0.1% formic acid (A) and acetonitrile containing 0.1% formic acid (B). We used a trap−elute configuration, including a trapping column (ChromXP C18-CL, 120 Å, 5 mm, 0.3 mm catridge; Eksigent Technologies) and an analytical column (ChromXP C18-CL, 120 Å, 150 × 0.3 mm^2, 5 mm; Eksigent Technologies) for peptide separation. A 6 μg sample of peptide was injected, trapped, and cleaned on the trapping column with mobile phase A at a flow rate of 10 μL/min for 3 min. The injected samples were then separated on the analytical column with gradient elution at a flow rate of 5 μL/min (Supplementary Table 2). Between each sample run,

https://doi.org/10.1021/acsptsci.1c00016
ACS Pharmacol. Transl. Sci. 2021, 4, 870−887

we injected a blank sample to minimize carryover. Ionization was achieved via positive ion mode with an ion spray voltage of 3000 V and a source temperature of 280 °C.

Drug Selection and Data Extraction. Nucleoside and nucleotide prodrugs with known activating enzymes or potential anti-SARS-CoV-2 activity were reviewed and categorized according to their prodrug types. TAF, sofosbuvir, remdesivir, and several other prodrugs have very similar prodrug structures consisting of the phenol and L-alaninate esters that serve as promoieties to mask the anionic phosphate moiety; this is termed the McGuigan prodrug design or ProTide technology.[27] We included three clinically approved ProTides: remdesivir, sofosbuvir, and TAF in the analysis. Isopropyl ester ProTides of GS-9148[28] and PSI-353661[29] were selected for evaluation because their structures are similar to those of sofosbuvir. GS-465124, GS-6620,[30] and GS2[31] were included because of their structural similarity to remdesivir: In the nucleoside moiety, these compounds differ from remdesivir only by a methyl group on the 2′ pentose ring. PSI-352938[32] and JNJ-54257099[33] are cyclic phosphate prodrugs. Valaciclovir and 5′-O-L-valyl-decitabine (L-val-DAC) were selected as examples of L-valyl ester prodrugs.[34] Laninamivir octanoate was selected as an example of a long-acting inhaled antiviral prodrug.[30] The activating enzymes and activation mechanisms of these prodrugs were obtained from the literature and carefully reviewed and scrutinized.[28,29,31−40]

Molecular Modeling. Favipiravir (T-705) has been approved for emergency treatment of COVID-19 in Russia and Japan due to its promising effects against SARS-CoV-2;[41,42] however, it may have several inherent issues in its activation that lead to a high dose requirement.[41,43] Aside from favipiravir, at the date of this writing, remdesivir is the only other anti-COVID-19 drug approved by a government agency. However, some researchers have argued that its nucleoside form, GS-441524, should replace remdesivir for the treatment of COVID-19 due to the observed limitations in remdesivir PK (e.g., low plasma stability).[11] In order to improve the PK performance of favipiravir and GS-441524, we propose two types of ester prodrugs for each: an isopropyl ester ProTide and an L-valyl-ester prodrug. Notably, the isopropyl ester ProTide form of GS-441524 (isopropyl-GS-441524) has been synthesized in a previous study and demonstrated much greater plasma stability than that of remdesivir ($t_{1/2}$: 1561 vs 69 min) in the *in vitro* human plasma incubations.[44] The $t_{1/2}$ of remdesivir in healthy human subjects were 54 and 63 min following a single IV dose of 75 and 225 mg, respectively.[45]

Structural Preparation of Ligands and Target Proteins. We used ChemDraw Professional 16.0 (PerkinElmer Informatics, Inc.) to sketch the 2D structures of valacyclovir, L-valyl-T-705, L-valyl-GS-441524, ProTide-T-705, isopropyl-GS-441524, and sofosbuvir. The 3D structures of all ligands were constructed and prepared using the LigPrep program implemented in the Schrodinger software suite (Maestro version 11.2). Possible ligand states at the target pH 7.0 ± 2.0 were generated by Epik, with specified chiralities retained for stereoisomer computation.

Crystal structures of the target proteins, including CES1, CTSA, BPHL, and PEPT1, were downloaded from the Research Collaboratory for Structural Bioinformatics Protein Data Bank (RCSB-PDB https://www.rcsb.org/). The corresponding PDB IDs of the crystal structures are 1YA4 (CES1, resolution 3.20 Å), 4CIA (CTSA, resolution 1.98 Å), 2OCI (BPHL, resolution 1.90 Å), and 4TPH (PEPT1, 3.15 Å). Except for BPHL with a monomer crystal structure, the other three proteins' crystal structures were nonmonomer, and their monomers were split from the original structures for further study. We applied the Protein Preparation Wizard in the Schrodinger software to prepare the target proteins for docking. The structures of the target proteins were preprocessed by adding hydrogens, creating disulfide bonds, deleting water molecules 5 Å beyond het groups, and generating het states at pH 7.0 ± 0.2. Missing side chains were filled. After adding hydrogens and deleting water, restrained minimization (hydrogen atoms only) was performed for each target protein to optimize the structure. Next, docking grid files were generated using the Receptor Grid Generation module. For each protein, the center of the docking site was specified by locating its cocrystallized ligand. The docked ligands were confined to an enclosing box with a side length of 20 Å.

Molecular Docking. Flexible ligand docking simulations were performed using the Glide module of the Schrodinger software (Maestro version 11.2).[46] The Glide docking settings were as follows: (1) the standard precision version of the docking scoring function; (2) a scaling factor and partial charge cutoff of 0.80 and 0.15, respectively; (3) the "sample nitrogen inversions" and "sample ring conformations" options for ligand sampling; (4) reward intramolecular hydrogen bonds and add Epik state penalties to docking scores; and (5) write out at most 15 poses per ligand and perform postdocking minimization.

Data Analysis. A label-free DIA-TPA method was used for quantitative proteomics analysis.[25] LC-MS/MS data were analyzed using Spectronaut 10.0 with a human proteome FASTA file downloaded from UniProtKB. Another FASTA file (Supplementary File 2) containing 238 human serine hydrolases was used to screen serine hydrolases from the proteome data obtained by above label-free DIA-TPA method. Other enzymes of interest were manually selected out using their UniPro IDs (available at UniProtKB). The enzyme$_i$ concentration (conc.) (pmole per mg S9 protein) in the S9 fraction of tissue$_j$ was calculated using eq 1. The concentration of enzyme$_i$ in a specific tissue was calculated by eq 2. The S9 fraction/tissue scaling factors were adopted from a previous study.[24] Data concerning the activities of purified recombinant human enzymes were extracted from the literature.[28,29,31,34−40] We used eq 3 to calculate each enzyme's contribution (contrib.) to the metabolism of a given substrate drug in a specific tissue, with an assumption that the activity of a recombinant (recomb.) enzyme was similar to that of its native counterpart in vivo.[24] Summation of the individual enzyme contributions in a specific tissue was then used to estimate the total metabolic activity in that tissue (eq 4). The calculation process was exemplified by sofosbuvir hydrolysis rate prediction as shown in Supplementary Table 3.

$$\text{Enzyme}_i \text{ conc. in tissue}_j \text{ S9} = \frac{\text{MS signal}(i)}{\text{Total MS signal}} \times \text{Total protein conc. of tissue}_j \text{ S9} \quad (1)$$

$$\text{Enzyme}_i \text{conc. in tissue}_j = \text{Enzyme}_i \text{ conc. in tissue}_j \text{ S9} \times \text{S9 conc. in tissue}_j \quad (2)$$

https://doi.org/10.1021/acsptsci.1c00016
ACS Pharmacol. Transl. Sci. 2021, 4, 870−887

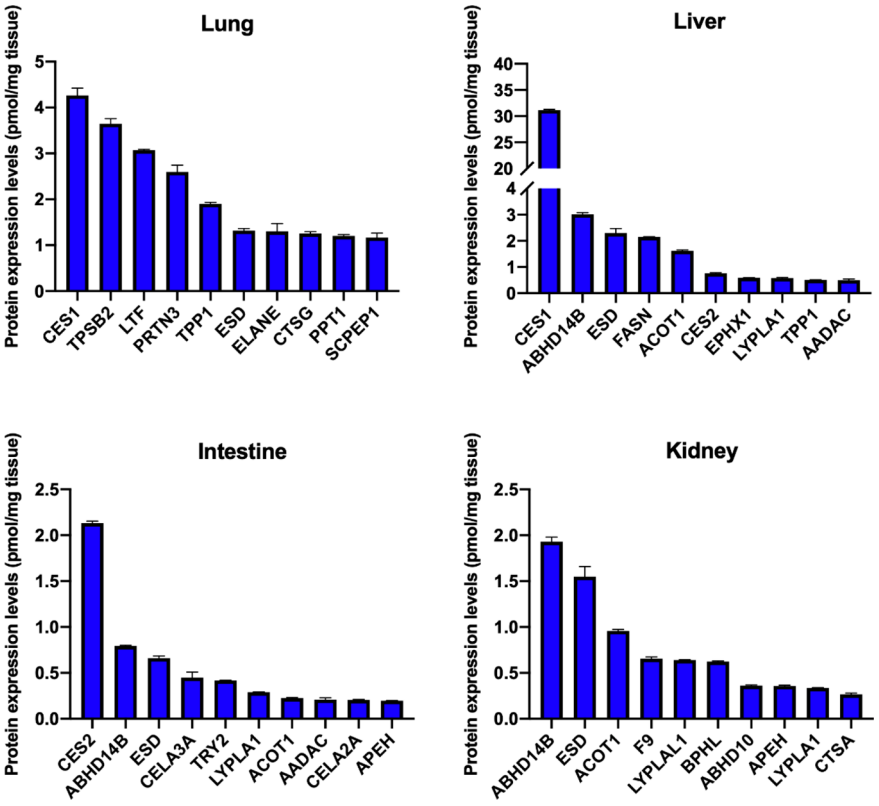

Figure 2. Protein abundance of the 10 most abundant serine hydrolases in the human lung, liver, intestine, and kidney. Data are the means of three independent measurements with error bars representing standard deviation (SD). Unit: pmol/mg tissue.

$$\text{Enzyme}_i \text{ contrib. in tissue}_j = \text{Recomb. human enzyme}_i \text{ activity} \times \text{Enzyme}_i \text{ conc. in tissue}_j \quad (3)$$

$$\text{Tissue}_j \text{ activity} = \sum \text{Enzyme}_i \text{ contrib. in tissue}_j \quad (4)$$

RESULTS

Abundance of Serine Hydrolases in the Human Lung, Liver, Intestine, and Kidney. The protein expression levels of the 10 most abundant serine hydrolases in the human lung, liver, intestine, and kidney were illustrated in Figure 2. A total of 71 serine hydrolases were detected in these human tissues and their abundance were displayed in the Supplementary Figure 1. The protein expression patterns of serine hydrolases showed significant differences between tissues. For example, CES1 was the most abundant hydrolase in the lung and liver but expressed at low levels in the intestine and kidney. In particular, CES1 abundance in the liver was approximately 7-fold higher than that in the lung. Meanwhile, CES2 was the most abundant serine hydrolase in the intestine, but its protein expression in the lung was very low.

Prediction of Prodrug Activation in Different Tissues. *ProTide.* We selected nine ProTides for activation analysis. Given that ProTides all undergo activation through similar intracellular enzymatic metabolism pathways, we used TAF to exemplify the activation process.[37,47,48] Once it enters a cell, TAF is hydrolyzed by several hydrolases (e.g., CES1 and CTSA) to cleave the ester group, followed by a series of rapid chemical steps that form the alanine metabolite. The P−N bond of the alanine metabolite is then cleaved by phosphoramidases (e.g., human histidine triad nucleotide-binding protein-1 [HINT1]) or via spontaneous acidic hydrolysis in lysosomes to liberate the monophosphate nucleoside (MP-Nuc). The MP-Nuc metabolite is further phosphorylated by host cell kinases to form the final active metabolite TP-Nuc (Figure 3a).

Enzyme activity and tissue stability data extracted from the literature are summarized in Table 1. Specifically, the *in vitro* human plasma half-life of remdesivir is significantly shorter than that of other ProTides. Meanwhile, GS2 exhibited a better intestinal S9 stability than other ProTides and also showed a better liver S9 stability than others except the isopropyl ester prodrug of GS-9148. CTSA showed much higher hydrolysis activity than CES1 for all ProTides, but its activity also differed significantly for different ProTides that shared the same ester moiety (isopropyl ester) but had different nucleoside cores. CTSA activities on the hydrolysis of sofosbuvir, TAF, and the GS-9148 isopropyl ester prodrug were greater than those on other evaluated ProTides.

Tissue expression levels of the major ProTide-hydrolyzing enzymes CES1, CTSA, and elastase (ELANE) are shown in Figure 3b. The CTSA protein level was highest in the lung, followed by the kidney, liver, and intestine. For CES1, protein abundance is ranked as follows: liver > lung > intestine > kidney. Finally, ELANE showed its highest expression in the lung and could be readily detected in the liver, but it was undetectable in the intestine and kidney.

The hydrolysis rates of six ProTides in the liver, lung, intestine, and kidney were calculated based on catalytic data from previous recombinant enzyme studies (Figure 3c).[28,29,31,37−39] The liver was found to have the highest hydrolysis activity for all selected ProTides except TAF and

https://doi.org/10.1021/acsptsci.1c00016
ACS Pharmacol. Transl. Sci. 2021, 4, 870−887

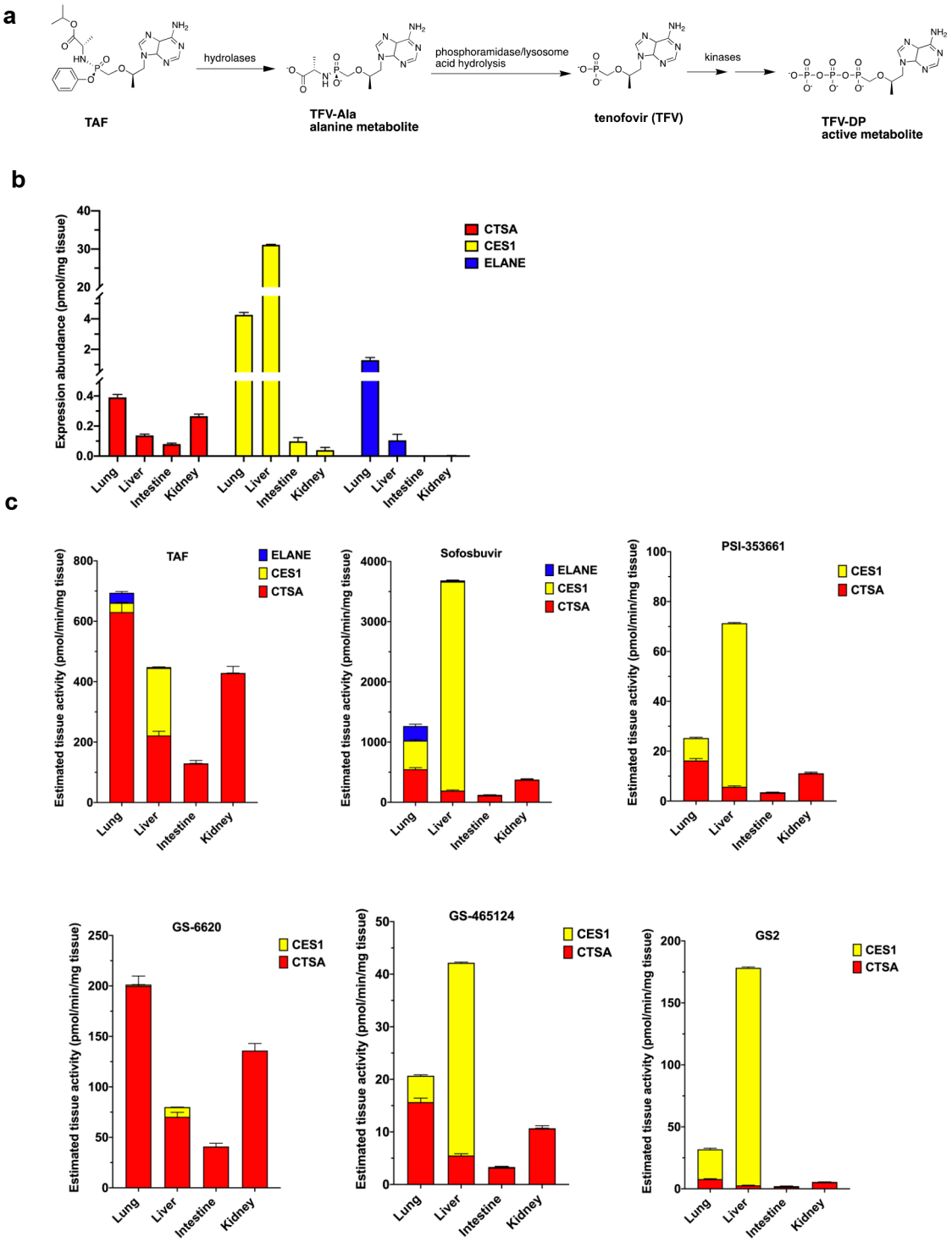

Figure 3. Hydrolysis efficiency of several ProTides in different human tissues. (a) Activation pathway of ProTides (taking TAF as an example).[37,47] (b) Protein expression of major activating enzymes CTSA, CES1, and ELANE in different human tissues. Data are the means of three independent measurements (n = 3). Colored bars represent mean values and error bars represent SD. (c) Estimated ester hydrolysis rate of prodrugs in different tissues. Colored bars represent mean values and error bars represent SD. TFV-Ala: tenofovir-alanine; TFV-DP: tenofovir diphosphate (TP-Nuc of TAF).

GS-6620. CES1 was the major enzyme contributing to the hepatic hydrolysis of sofosbuvir, GS-465124, PSI-353661, and GS2, but it may play a minor role in hepatic hydrolysis of GS-6620. In the lung, the hydrolysis rates of these ProTides ranked as follows: sofosbuvir > TAF > GS-6620 > GS2 > PSI-353661 > GS-465124. CTSA played a major role in the pulmonary hydrolysis of TAF, GS-6620, PSI-353661, and GS-465124; it was also the major contributor to intestinal and renal hydrolysis of these ProTides. Both catalytic activity and protein abundance of the activating enzyme should be taken into consideration when evaluating the contribution of an enzyme to prodrug activation. For instance, although CTSA exhibited a much higher catalytic activity on cleaving the GS-465124 ester bond than CES1,[39] the significantly higher

https://doi.org/10.1021/acsptsci.1c00016
ACS Pharmacol. Transl. Sci. 2021, 4, 870−887

Table 1. Recombinant Enzyme Activity, Hepatic and Intestinal S9 Stability, and Plasma Stability of ProTides[a]

prodrug	log D or log P[a]	passive diffusion?[c]	human recombinant enzyme activity (pmol/min/μg)[b] CTSA	CES1	ELANE	human intestinal S9 $t_{1/2}$ (min)	human hepatic S9/ hepatocytes $t_{1/2}$ (min)	human plasma $t_{1/2}$ (min)[d]	ref
GS-7340 (TAF)	1.6	yes	31000	116[e]	891	33.5	18	116.9	37,47,48
GS-7977 (sofosbuvir)	1.62	n.a.	27000	1800	6500	n.a.	34.2	>1440	38,49
isopropyl ester ProTide of GS-9148	2.16	n.a.	35000	n.a.	n.a.	106	159	*f*	28
PSI-353661	n.a.	n.a.	800	34	n.a.	n.a.	12	>1440	29,50
GS-465124	n.a.	n.a.	770	19	n.a.	261	5.3	360	39
GS-6620	n.a.		9834[g]	5	n.a.	17	4	371	39
GS2	n.a.		385	91	n.a.	570	87	>600	31
GS-5734 (remdesivir)	2.1	n.a.	n.a.	n.a.	n.a.	n.a.	n.a.	69	44
isopropyl-GS-441524	1.1	n.a.	n.a.	n.a.	n.a.	n.a.	n.a.	1561	44

[a]Data from available literature. Data for TAF and sofosbuvir are reported as log P (octanol/water partition coefficient), which were obtained from PubChem (https://pubchem.ncbi.nlm.nih.gov). [b]CES1: carboxylesterase 1; CTSA: cathepsin A; ELANE: elastase. Activity is represented as pmol compound cleaved/min/μg of recombinant human enzymes or pmol alanine metabolite formed/min/ug of recombinant human enzymes. [c]n.a.: Data were not found by the authors. [d]All $t_{1/2}$ data were obtained from *in vitro* human plasma incubations except for the isopropyl ester ProTide of GS-9148,[28] which was incubated in dog plasma *in vitro*. The concentrations of different substrates may be different during incubation. The plasma incubation concentrations of TAF,[47] remdesivir,[44] isopropyl-GS-441524,[44] GS2,[31] GS-6620,[39] and GS-465124[39] were 2 μM, while that of sofosbuvir[49] was 100 μM. The incubation concentration of PSI-353661 was unavailable.[50] [e]The activity of porcine liver carboxylesterase, which was considered as a close homologue of human CES1 in the original study.[37] [f]The isopropyl ester prodrug of GS-9148 was 100% remaining after 1 h of dog plasma incubation.[28] [g]Only the CES1 activity for amidate ester cleavage, without including the CES1 activity for 3′-ester cleavage.

hepatic CES1 expression compared to CTSA makes CES1 the primary GS-465124 activating enzyme in the liver.

Cyclic Monophosphate Prodrug. PSI-352938 and JNJ-54257099 adopt the cyclic monophosphate prodrug technology, which can form the MP-Nuc metabolites directly through their activation pathways, bypassing the first phosphorylation step. Both prodrugs were originally developed as orally dosed anti-HCV drugs. Their activations were initiated by the removal of the isopropyl group in the cyclic phosphate moiety, which was mainly catalyzed by cytochrome P450 3A4 (CYP3A4) (Figure 4a).[32,33] The activities of CYP3A4 on PSI-352938 and JNJ-54257099 were calculated to be 2.27 and 1.32 pmol/min/pmol of CYP3A4, respectively, based on the intrinsic clearance reported in a previous study.[33] The original study of PSI-352938 tested 16 hydrolases (e.g., CESs, cathepsins, and lipase) and multiple CYPs, and it identified CYP3A4 as the only enzyme involved in the initial activation of the prodrug.[32] Here, we determined the protein expression levels of CYP3A4 in human lung, liver, intestine, and kidney (Figure 4b) and estimated the rates of the CYP3A4-catalyzed isopropyl group removal, the initial activation step of the prodrugs (Figure 4c). CYP3A4 is abundant in the liver and intestine but barely detectable in the lung and kidney. The abundance of CYP3A4 in the liver was approximately 2-fold higher than that in the intestine; thus, the activation rates of these prodrugs in the liver were estimated to be approximately 2-fold higher than in the intestine. PSI-352938 and JNJ-54257099 are predicted to be barely activated in the human lung and kidney because of the extremely low expression levels of CYP3A4 in these tissues.

L-Valyl Ester Prodrugs. Valacyclovir and L-val-DAC were selected as representative L-valyl ester prodrugs. Valacyclovir can be efficiently transported across the intestinal epithelium membrane by the human intestinal peptide transporters oligopeptide transporter 1 (PEPT1) and peptide-associated transporter 1 (HPT1); this transport significantly improves its bioavailability relative to acyclovir.[51−54] Valacyclovir has been demonstrated a substrate of the intestinal hydrolase biphenyl hydrolase-like protein (BPHL), which recognizes its L-valyl ester structure.[55] A recent proteomics study identified another hydrolase capable of activating valacyclovir, namely, retinoblastoma-binding protein 9 (RBBP9).[36] L-val-DAC is also a substrate of BPHL and PEPT1 and features significantly improved bioavailability and rapid intestinal activation.[34,56] The activity of BPHL on L-val-DAC (91 600 pmol/min/μg) was extracted from the V_0 versus [S] plot of BPHL-mediated L-val-DAC hydrolysis reported in a previous study.[34] The activities of BPHL and RBBP9 on valacyclovir have been reported as 68 000[35] and 47 960[36] pmol/min/μg, respectively. The ester hydrolysis pathway of these two prodrugs is illustrated in Figure 5a, while the observed abundances of the transporters PEPT1 and HPT1 and the enzymes BPHL and RBBP9 in various tissues are shown in Figure 5b. PEPT1 and HPT1 were mainly expressed in the intestine. Lung BPHL expression was comparable to that observed in the intestine but lower than in the liver and kidney; expression levels of RBBP9 were comparable in the lung, liver, and kidney but were much lower in the intestine. The predicted hydrolytic activity of valacyclovir and L-val-DAC in different tissues is shown in Figure 5c. The intestinal hydrolysis rates of the two L-valyl ester prodrugs were comparable to their pulmonary hydrolysis rates but lower than their hepatic and renal hydrolysis rates.

Long-Lasting Inhaled Prodrug. Laninamivir octanoate is a long-lasting neuraminidase inhibitor for the treatment of influenza.[30] Lysophospholipase 1 (LYPLA1) and esterase D (ESD) were identified as the major enzymes responsible for hydrolysis of laninamivir octanoate in human lung S9 fractions, with catalytic activities of 0.377 and 0.232 pmol/min/μg of enzyme, respectively.[40] The pulmonary expression of ESD was comparable to its renal expression and higher than its intestinal expression, but it was lower than the liver expression. Meanwhile, LYPLA1 levels in the lung were comparable to those in the intestine but slightly lower than levels in the liver and kidney. In all tissues, the estimated ester hydrolysis of

https://doi.org/10.1021/acsptsci.1c00016
ACS Pharmacol. Transl. Sci. 2021, 4, 870−887

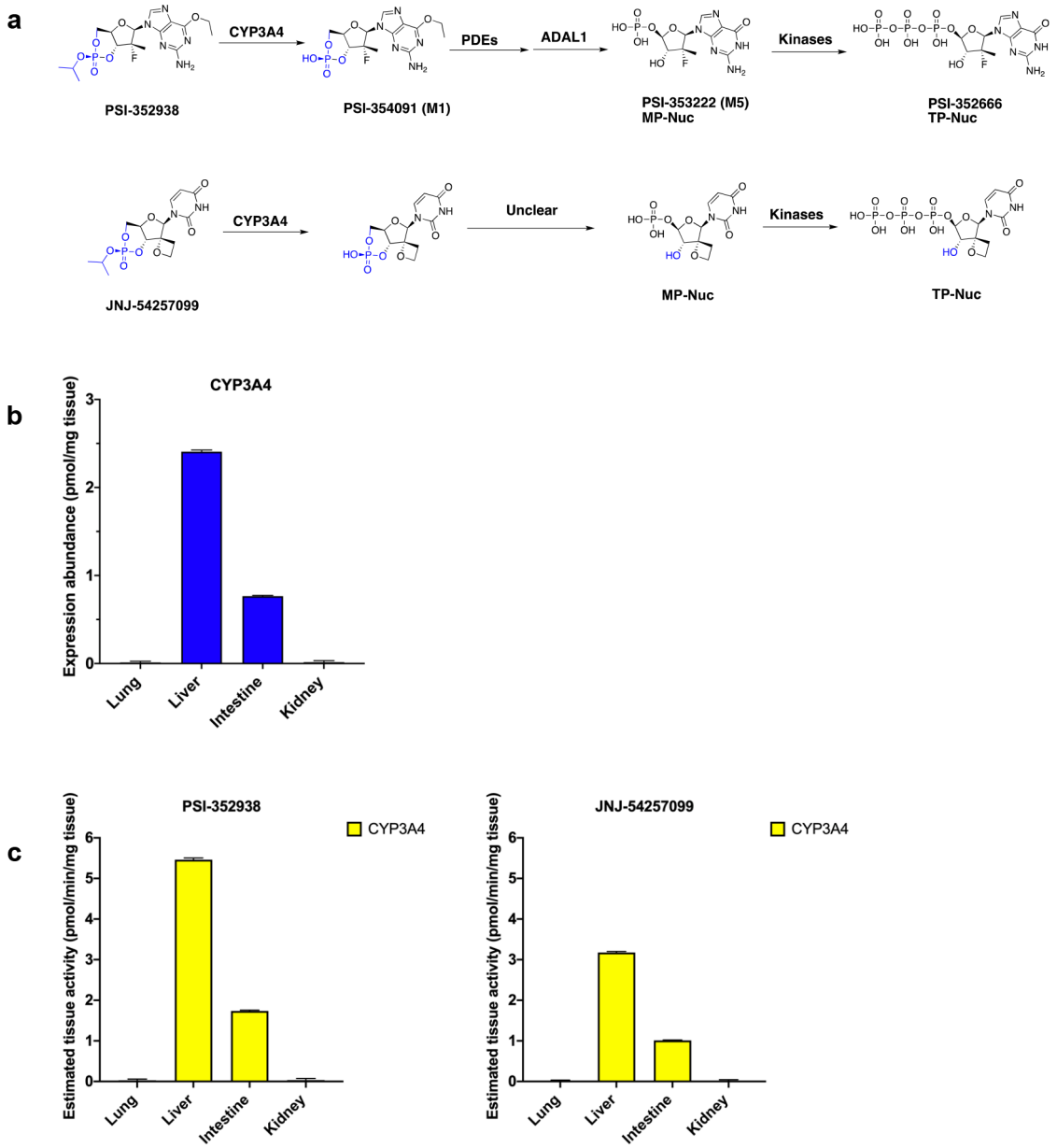

Figure 4. Hydrolysis efficiency of two cyclic monophosphate prodrugs. (a) Putative the activation pathway of PSI-352938 and JNJ-54257099.[32,33] (b) Protein expression of CYP3A4 in different human tissues. Data are the means of three independent measurements with error bars representing SD. (c) Estimated ester hydrolysis rate of prodrugs in different tissues. Colored bars represent mean values and error bars represent SD. CYP3A4: cytochrome P450 3A4; PDEs: phosphodiesterases.

laninamivir octanoate was relatively slow, ranging from 0.0075 to 0.022 pmol/min/mg of tissue (Figure 6).

Prodrug Design and Docking Study. We proposed two types of prodrugs for improving the PK properties of favipiravir and GS-441524 (Figure 7a). We used the ProTide technology to modify T-705-ribonucleoside (T-705-R) and GS-441524, yielding isopropyl-alanyl phosphamide prodrugs ProTide-T-705-R and isopropyl-GS-441524. In addition, we added an L-valyl group to the 5′-T-705-R and GS-441524 to form L-valyl ester prodrugs L-valyl-705-R and L-valyl-GS-441524. To evaluate whether the proposed prodrugs have merits in terms of high susceptivity to the corresponding activating enzymes or transporters, we performed a computational docking experiment; the binding modes of the prodrugs in stereoview are displayed in Figure 7b,c. Calculated binding energies obtained for specific activating enzymes (esterases) and transporters by docking the prodrug molecules into the protein-binding pocket are listed in Table 2. The calculated binding energies of CES1 and CTSA complexed with ProTide-T-705-R were comparable to those for sofosbuvir, whereas isopropyl-GS-441524 was shown to have a 2.40 kcal/mol lower docking score to CTSA and a 2.99 kcal/mol higher docking score to CES1 than sofosbuvir, suggesting a CTSA preference for isopropyl-GS-441524. Additionally, the calculated binding energies of PEPT1 and BPHL complexed with L-valyl-T-705-R and L-valyl-GS-441524 were generally comparable to those for valacyclovir.

Moreover, we visualized the binding modes of the proposed prodrugs with the candidate enzymes and transporter (Figure 7b,c). Since the catalytic mechanisms (nucleophilic attacking) of CES1, CTSA, and BPHL have been reported by previous studies with the key catalytic residues being identified as

https://doi.org/10.1021/acsptsci.1c00016
ACS Pharmacol. Transl. Sci. 2021, 4, 870−887

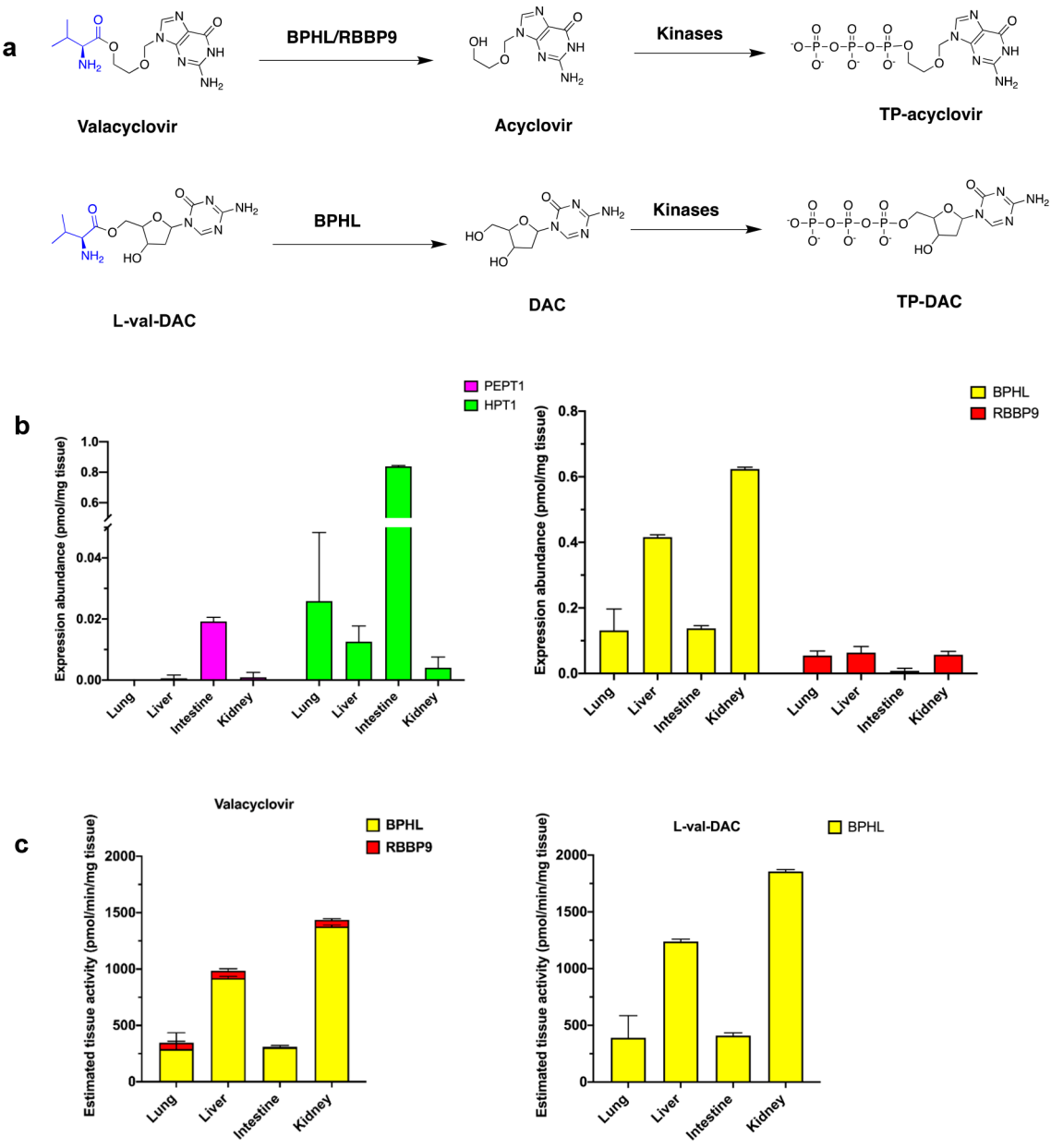

Figure 5. Hydrolysis efficiency of valacyclovirr and L-val-DAC in different human tissues. (a) Activation pathway of valacyclovir and L-val-DAC.[34−36] The blue color highlights the L-valyl ester structure. (b) Protein expression of the transporters PEPT1 and HPT1 and the enzymes BPHL and RBBP9 in different tissues. (c) Estimated tissue activity for the ester hydrolysis of valacyclovir and L-val-DAC. Data are the means of three independent measurements with error bars representing SD. PEPT1: peptide transporters oligopeptide transporter 1; HPT1: human peptide-associated transporter 1; BPHL: biphenyl hydrolase-like protein; RBBP9: retinoblastoma-binding protein 9.

SER221,[57] SER150,[58] and SER122,[34] respectively, we selected the docking pose of the prodrugs to visualize where the ester carbonyl of the prodrugs located closely to the oxhydryl of the corresponding serine residue. For the interaction between L-valyl ester prodrugs and PEPT1, GLU402 was reported as the key residue forming the hydrogen bond to the amino group on the ester structure of L-val-DAC.[56] All the top docking poses appear acceptable from the mechanism perspective except for isopropyl-GS-441524 with CES1, for which we depicted its top 2 docking poses that matched the putative interaction. Our proposed prodrugs may form several polar contacts with the residues at the binding sites of these proteins, which may contribute to the binding affinities. Overall, our molecular docking simulation demonstrated that the proposed prodrugs were likely to be catalyzed by these specified proteins.

DISCUSSION

Prodrug activation is a major determinant of the intracellular concentration of TP-Nuc, which is directly associated with the therapeutic effects of anti-SARS-CoV-2 prodrugs. Ester prodrug activation requires an initial enzymatic cleavage of the ester group, which is critical for the whole activation process. The efficiency of this activation step is dependent on the catalytic activity and abundance of the responsible hydrolases. The lung, liver, intestine, and kidney are the primary sites for human drug metabolism, with the lung being the major site of action for COVID-19. Therefore, profiling the protein expression of activating enzymes in these tissues is essential for understanding the PK and anti-COVID-19 effects of antiviral ester prodrugs. In the present study, we identified

https://doi.org/10.1021/acsptsci.1c00016
ACS Pharmacol. Transl. Sci. 2021, 4, 870−887

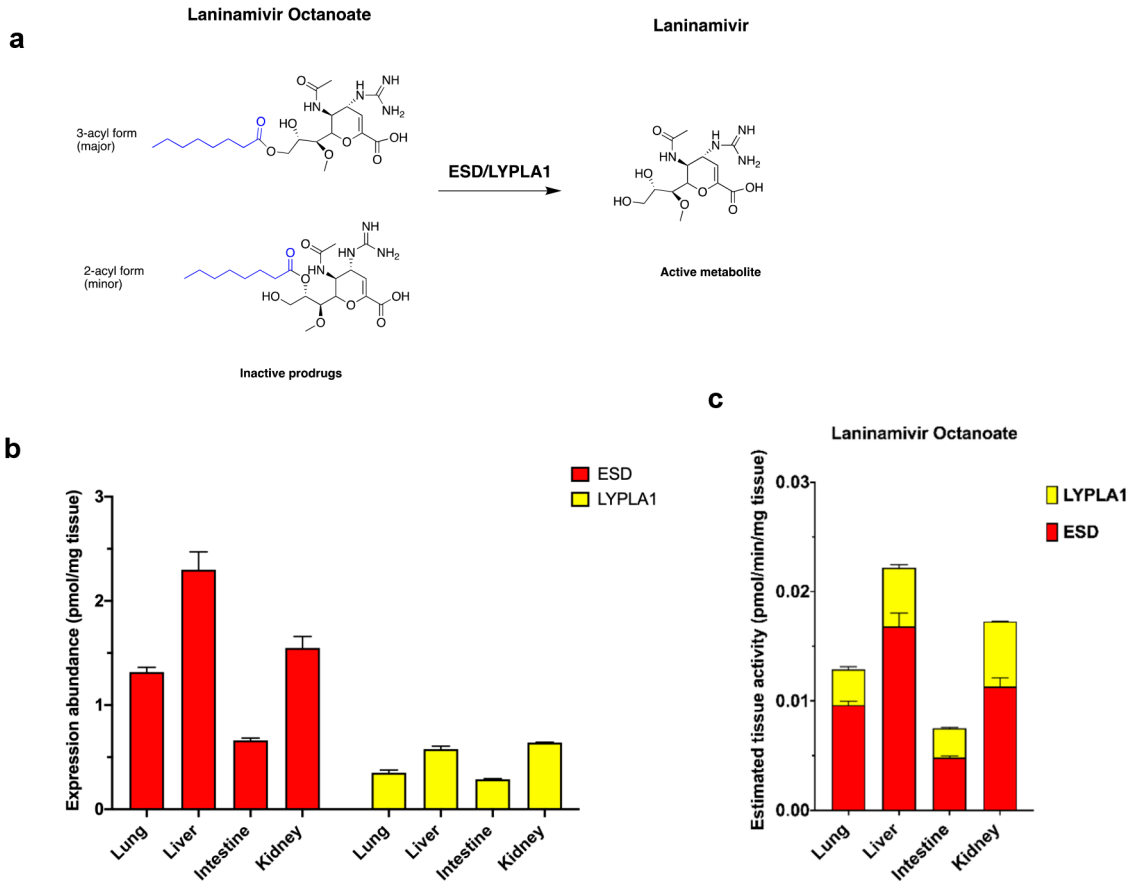

Figure 6. Hydrolysis efficiency of laninamivir octanoate in different human tissues. (a) Activation pathway of laninamivir octanoate activation.[40] (b) Protein levels of ESD and LYPLA1. (c) Predicted ester hydrolysis rate of laninamivir octanoate in different tissues. Data are the means of three independent measurements with error bars representing SD. ESD: esterase D; LYPLA1: lysophospholipase 1.

tissue-dependent activation profiles for many antiviral prodrugs based on the abundance and activity of activating enzymes in different tissues. The results indicated that designing prodrugs to target specific activating enzymes abundant in the target tissue could improve the antiviral effect at the target site and reduce the prodrug's off-target effects. Our study thus leads to recommendations for the future development and application of anti-COVID-19 prodrugs (Table 3).

Admittedly, the materials (i.e., tissue S9 fractions) used in the proteomics analysis may carry a potential limitation. Although S9 fractions are a good representation of the overall proteome of a tissue of interest, the tissue may contain different types of cells with distinct protein expression profiles. For example, lung tissue contains multiple types of cells, such as type I (AT1), type II alveolar epithelial cells (AT2), macrophages, and capillary endothelial cells. The protein expression patterns of prodrug-activating enzymes could differ significantly among these cells. SARS-CoV-2 has been indicated to mainly infect AT2 cells,[59] which comprise a relatively small fraction of the total lung cells[60] and do not express CES1 and CTSA at high levels. According to The Human Protein Atlas (www.proteinatlas.org), the expression levels of CTSA and CES1 in AT2 cells are approximately 2-fold and 3- to 9-fold lower, respectively, than those in the macrophages. As such, the ProTides bioactivation efficacy predicted based on the expression levels of activating enzymes in the whole lung may have been overestimated. Thus, *in situ* cellular metabolism profiling may offer additional insights into prodrug activation in the sites of action and their anti-SARS-CoV-2 efficacy.

Nine ProTides were selected for the analysis: Sofosbuvir and TAF were included because they have been approved for use in the clinic and have shown anti-SARS-CoV-2 efficacy in *in vitro* studies.[4,7] Isopropyl ester ProTides of GS-9148[28] and PSI-353661[29] were selected because their structures are very similar to sofosbuvir and have shown promising anti-HIV and anti-hepatitis C virus (HCV) effects *in vitro*, respectively. GS-465124, GS-6620,[30] and GS2[31] were included because of their structural similarity to remdesivir in the nucleoside core, which may render their anti-SARS-CoV-2 effects. Among these nine ProTides, two belong to the phosphonate prodrug class, namely, TAF and the isopropyl ester ProTide of GS-9148, while the other seven are phosphate prodrugs. The activity of CTSA on metabolizing these two phosphonate prodrugs were generally higher than that for phosphate prodrugs (Table 1). Whether this is because of the structure−activity relationship or interstudy variance remains to be determined. It appears plausible that increasing the CTSA preference may be favorable for the pulmonary activation of prodrugs given the relatively higher CTSA expression level in the lung. Importantly, our results suggested that the liver was the primary site of activation for most oral antiviral ProTides. Most antiviral ProTides, such as sofosbuvir and TAF, were initially designed for the treatment of hepatitis B virus (HBV) and hepatitis C virus (HCV) infections. In these contexts, extensive hepatic activation is considered an advantage because it allows

https://doi.org/10.1021/acsptsci.1c00016
ACS Pharmacol. Transl. Sci. 2021, 4, 870−887

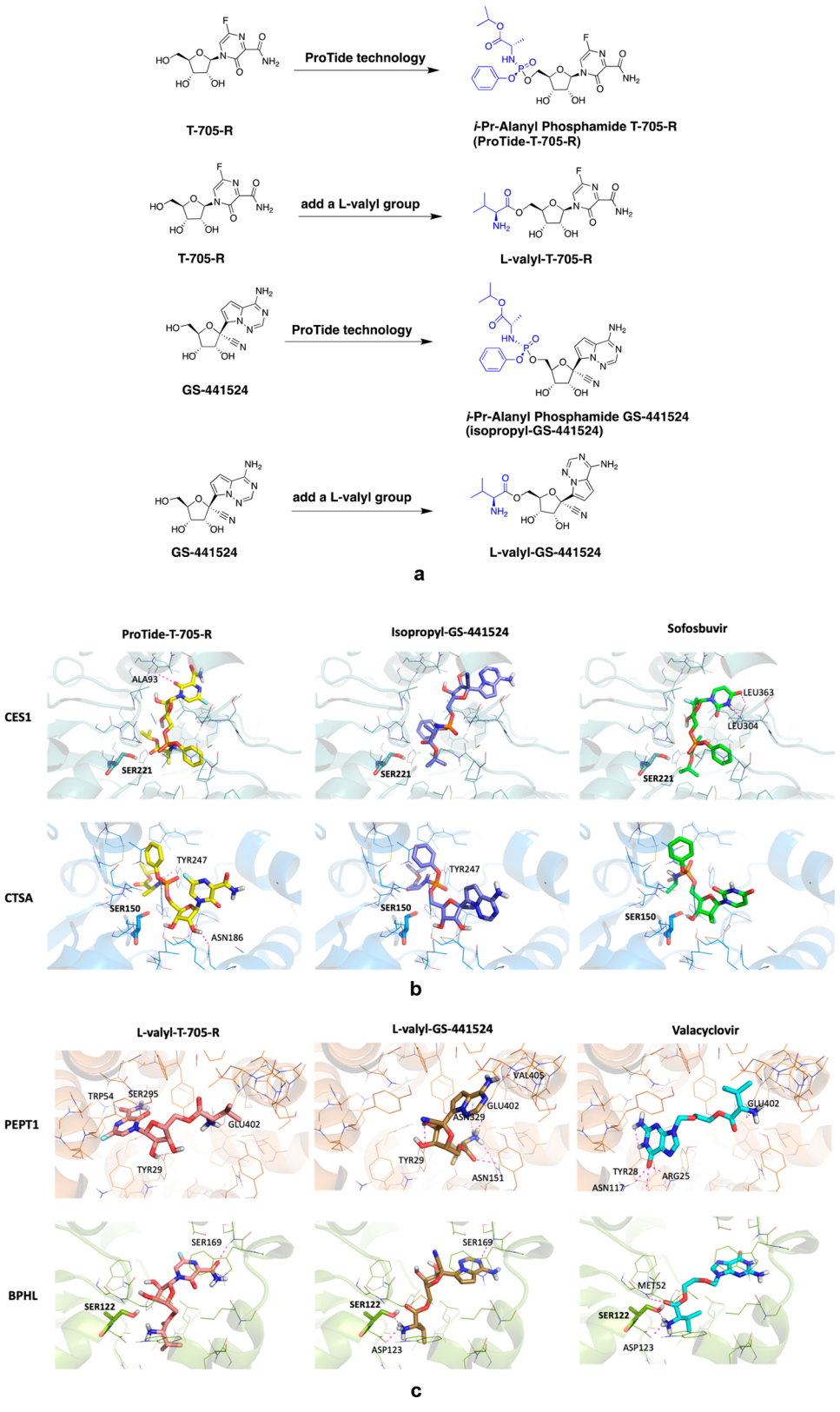

Figure 7. Prodrug design of favipiravir and GS-441524. (a) Proposed ProTide and L-valyl ester prodrugs of favipiravir and GS-441524. ProTide technology was used to modify T-705-ribonucleoside (T-705-R) and GS-441524 to form the isopropyl-alanyl phosphamide prodrugs: ProTide-T-705-R and isopropyl-GS-441524. A L-valyl group was added as the masking group to the 5′-T-705-R and GS-441524 to form the L-valyl ester prodrugs L-valyl-705-R and L-valyl-GS-441524. (b) Interactions between the binding-site residues of CES1 (PDB ID: 1YA4) and CTSA (PDB ID: 4CIA) and the ligands of ProTide form ProTide-T-705-R, isopropyl-GS-441524, and sofosbuvir. (c) Interactions between the binding-site residues of PEPT1 (PDB ID: 4TPH) and BPHL (PDB ID: 2OCI) and the ligands of L-valyl ester prodrugs L-valyl-T-705-R, L-valyl-GS-441524, and valacyclovir. Ligands are shown as sticks and colored by elements. Proteins are represented as cartoons, and residues at binding sites are shown in lines and colored by elements. Polar contacts formed between ligands and proteins are shown in the dashed magenta lines.

https://doi.org/10.1021/acsptsci.1c00016
ACS Pharmacol. Transl. Sci. 2021, 4, 870−887

Table 2. Calculated Binding Free Energies (kcal/mol, Docking Scores) of Specific Activating Enzymes and Transporters Complexed with Designed Prodrugs

prodrug type	protein	proposed prodrug		control prodrug
		favipiravir (T-705)	GS-441524	
ProTide		ProTide-T-705-R[a]	isopropyl-GS-441524	sofosbuvir
	CES1	−8.12	−5.16	−8.25
	CTSA	−7.84	−9.26	−6.86
L-valyl ester prodrug		L-valyl-T-705-R	L-valyl-GS-441524	valacyclovir
	PEPT1	−6.15	−5.68	−6.06
	BPHL	−7.99	−7.23	−7.60

[a]T-705-R: T-705-ribonucleoside.

for rapid TP-Nuc formation in hepatocytes and the consequent exertion of antiviral effects in the liver. However, when prodrugs are used for COVID-19 treatment, the lung becomes the primary target; thus, oral dosing may no longer be desirable because of the extensive hepatic activation that results. This may partially explain why orally dosed sofosbuvir did not bring significant benefits to patients with COVID-19 after 1 week of treatment.[61] Therefore, we suggest that when sofosbuvir, TAF, and other antiviral ProTides are repurposed for COVID-19 treatment, parenteral dosing such as inhalation or IV infusion should be adopted to circumvent the extensive hepatic first-pass effect.

Ester prodrugs usually have significantly improved cell permeability relative to that of their nucleotide forms due to a neutrally charged structure and high lipophilicity. From this perspective, drug delivery to the action site can be improved with a prodrug that is able to remain intact in its prodrug form until after reaching the target cells. Therefore, for IV-dosed antiviral prodrugs such as remdesivir, increasing plasma stability could improve drug accumulation in pulmonary cells and thus enhance efficacy for COVID-19 therapy. However, our data analysis (Table 1) showed that remdesivir had lower plasma stability compared to other ProTides evaluated in this study. This could be attributed to the choice of ester group in each ProTide's design. Most ProTides, such as TAF and sofosbuvir, use isopropyl as the ester group, while remdesivir adopts the 2-ethylbutyl (2-EtBu) structure. According to a recent human PK study, after a single IV dose of remdesivir, its nucleoside form, GS-441524, becomes the predominant metabolite in the plasma with $t_{1/2}$ > 24 h.[45] Some researchers have argued that a large portion of remdesivir could be hydrolyzed by serum or hepatic esterase before reaching the lung, causing GS-441524 to be the predominant metabolite to which pulmonary cells are exposed.[11] When developing a prodrug, researchers usually test different ester structures for use as the masking moiety; changing the ester structure could change the prodrug's plasma stability.[28,44] During remdesivir development, several GS-441524 ester prodrugs were synthesized and evaluated for their plasma stability and antiviral activity in Hela cells, TERT-immortalized human foreskin microvascular endothelial cells (HMVEC), and human macrophage cells.[44] Remdesivir was chosen as the drug candidate because of its superior antiviral activity relative to other prodrugs. Among the tested prodrugs, the isopropyl ester ProTide of GS-441524 (isopropyl-GS-441524) showed relatively lower antiviral potency but much greater plasma stability than remdesivir ($t_{1/2}$: 1561 vs 69 min).[44] The *in vivo* human plasma $t_{1/2}$ of remdesivir was also short, with the mean value being 54 and 63 min after IV administration of single doses of 75 and 225 mg, respectively.[45] Notably, the differences in antiviral activity among the tested GS-441524 prodrugs are solely attributed to differences in their intracellular accumulation and activation rates because they all share the identical active metabolite. Our docking results showed that the isopropyl-GS-441524 prodrug appears to be a specific substrate for CTSA and CES1. Our quantitative proteomic analysis revealed that both CES1 and CTSA are highly expressed in the human lung (Figure 3b), indicating that the isopropyl-GS-441524 prodrug could be efficiently activated in the lung. Therefore, the isopropyl-GS-441524 prodrug warrants further investigation for its anti-COVID-19 effect.

Generally, MP-Nuc formation is a slow rate-limiting step in the activation of nucleoside analogs.[62] Phosphate/phosphonate prodrugs are often made by adding an ester group to the monophosphate structure, allowing for the first phosphorylation step to be bypassed and the MP-Nuc metabolite to be formed after cleavage of the ester group. This design

Table 3. Inspirations for the Nucleoside/Nucleotide Analog Prodrug Design for COVID-19 Treatment[a]

prodrug type	examples	original indication	original target site	dosing route	major activation site	ideas for COVID-19 drug development and applications
ProTide	TAF	HBV/HIV	liver/ PBMCs	oral	liver	Parenteral dosing is recommended in order to bypass the extensive first-passing effect in the liver; this may be helpful when the first phosphorylation is the rate-limiting step in the activation. Increasing the plasma stability may be favorable for pulmonary loading.
	sofosbuvir	HCV	liver			
	PSI-353661					
	GS-6620/ GS-465124					
	GS2					
	remdesivir	Ebola virus	PBMCs	IV infusion		
cyclic monophosphate prodrug	PSI-352938	HCV	liver	oral	liver	This may be not suitable for COVID-19 because their activating enzyme CYP3A4 is deficient in the lung.
	JNJ-54257099					
L-valyl ester prodrug	valacyclovir	HSV	genital	oral	intestine and liver	It is possible to improve the oral bioavailability of parent nucleoside form, especially when the first phosphorylation is not the rate-limiting step in the activation; May be capable of targeting intestinal SARS-CoV-2.
	L-val-DAC	cancer	tumor			
octanoate prodrug	laninamivir octanoate	influenza virus	lung	inhalation	lung	example of long-acting inhaled antiviral prodrug

[a]PBMCs: peripheral blood mononuclear cells; HSV: herpes simplex virus.

https://doi.org/10.1021/acsptsci.1c00016
ACS Pharmacol. Transl. Sci. 2021, 4, 870−887

contributes significantly to prodrugs having greater antiviral efficacy than their parent nucleoside forms.[19,44] For multiple phosphate/phosphonate prodrugs, efficient cellular absorption and rapid formation of the active metabolite TP-Nuc have been commonly observed in primary human hepatocytes.[16,29,32,38,39] One of the strategies is cyclic monophosphate prodrugs. PSI-352938 and JNJ-54257099 are two cyclic monophosphate prodrugs and both of them undergo the CYP3A4-mediated cleavage of their isopropyl group to form the MP-Nuc.[32,33] PSI-352938 and JNJ-54257099 were originally designed as oral prodrugs. Our results showed that these two prodrugs were mainly hydrolyzed in the liver and intestine, suggesting that this type of prodrug may not be ideal for COVID-19 treatment because the human lung lacks CYP3A4 to activate them. In contrast, our results revealed that the human lung has expression levels of serine hydrolases (e.g., CTSA and CES1) relatively higher than those in the liver (except CES1), intestine, and kidney for the activation of another type of monophosphate prodrug, ProTides. Of note, cautions should be exercised when adopting ProTides for the development of prodrugs against COVID-19. One potential limitation is that the whole lung tissue proteomics data we used may overestimate the AT2 cells' ability of activating ProTides since AT2 cells comprise a small fraction of the total pulmonary cells and express relatively lower abundance of CTSA and CES1 than other types of pulmonary cells. Moreover, our analysis focused on the initial activation step of ProTides, the ester hydrolysis. After cleavage of the ester group, the carboxylate intermediate metabolite undergoes further rapid chemical steps to form the alanine metabolite. The alanine metabolite then requires deamination to cleave the P−N bond and release the MP-Nuc. This step was believed to be catalyzed by HINT1 and, to a lesser extent, HINT2.[38,63,64] The abundance of HINT1 and HINT2 in various tissues is given in Supplementary Figure 1; most notably, the pulmonary expression of HINT1 was approximately half of its hepatic expression. However, previous evidence has indicated that conversion of the alanine metabolite to MP-Nuc for several ProTides might not necessarily depend on HINT1. For example, the P−N bond cleavage of TAF−Ala could be spontaneous in the acidic environment of a lysosome (pH 4.5), which is where the ProTide hydrolyzing enzyme CTSA is mainly expressed and the site of alanine metabolite is formed.[65] An *in vitro* study on sofosbuvir also found that HINT1 was not the sole catalyzing factor for converting its alanine metabolite to MP-Nuc.[38] As such, whether the relatively low HINT1 abundance in the lung would limit ProTide prodrug activation requires further investigation. Although MP-Nuc requires two additional phosphorylation steps to form the final active metabolite TP-Nuc, the formation of MP-Nuc is most critical due to the phosphate metabolites (MP-Nuc, DP-Nuc, and TP-Nuc) having low cell permeability on account of their multiple negative charges. Thus, once MP-Nuc is formed in a cell, the metabolite is likely to be trapped in the intracellular space, allowing for its efficient conversion to TP-Nuc by kinases. As such, the ester hydrolysis and the metabolism from alanine metabolite to MP-Nuc are the most essential steps for ProTide activation. However, recent findings showed that compared with remdesivir, GS-441524 had a stronger anti-SARS-CoV-2 efficacy in Vero E6 cells but a weaker efficacy in Calu-3[5,66] and Caco-2 cells.[5,66] Whether GS-441524 or isopropyl-GS-441524 can be more effective for COVID-19 treatment than remdesivir warrants further *in vivo* investigations.

Aside from having relatively low drug concentrations in the lung, another limitation of remdesivir is that the drug is currently only available in an IV dosage form and must be administered in an in-patient setting. Some efforts are being made to develop an inhalation formulation of remdesivir,[67] aiming to increase drug loading in the respiratory system. The inhalation formulation will also be more accessible for outpatients, offering an opportunity to treat COVID-19 during the early stage of infection. In addition, optimizing the prodrug structure should also be considered during the development of an inhalation formation, especially in the interest of achieving a long-lasting anti-SARS-CoV-2 effect. One example is the inhaled prodrug laninamivir octanoate, a long-acting neuraminidase inhibitor for the treatment of influenza.[30] After a single inhalation of 160 mg prodrug, its active metabolite laninamivir can maintain a concentration > EC_{50} in the epithelial lining fluid (ELF) for 164 h.[30] Moreover, at its standard dosage (40 mg daily), it showed a favorable safety profile and was effective in the Japanese population.[68,69] Our analysis indicated that hydrolysis of laninamivir octanoate in the lung and other tissues was very slow, at least 100-fold lower than for other types of prodrugs. The $t_{1/2}$ values reported for laninamivir octanoate in human alveolar macrophages and epithelial lining fluid were approximately 41 and 70−90 h, respectively.[30] This long $t_{1/2}$ supports our prediction that laninamivir octanoate has a slow hydrolysis rate in the lung. The long-lasting antiviral effect of laninamivir octanoate can be partially explained by the high dosage loading used (40−160 mg per inhalation) and its slow pulmonary hydrolysis. ESD and LYPLA1 are the major enzymes for the ester hydrolysis of laninamivir octanoate, and have much lower hydrolysis activity for this prodrug than is observed for CTSA hydrolyzing ProTides or BPHL hydrolyzing L-valyl ester prodrugs.[40] The *O*-octanoyl ester linkage on the structure of laninamivir octanoate, similar to that of sialic acid, may account for the specificity and susceptivity of this prodrug to ESD and LYPLA1,[40] so it may offer a reference for developing long-lasting inhaled antivirals for COVID-19 treatment.

Although the human lung is considered the primary site of the SARS-CoV-2 infection, increasing evidence suggests that extrapulmonary infections, such as of the intestine, are imperative for COVID-19 treatment outcomes.[70] It has also been recommended that antivirals should be given as early as possible after being infected with SARS-CoV-2.[71] However, the IV formulation of remdesivir limits its outpatient application in those who are at an early stage of COVID-19 and have mild symptoms. An oral antiviral drug can be a preferred option for this cohort and offers the benefit of eradicating the virus within the gastrointestinal system, thereby preventing feces−oral spread. Valacyclovir[72] and L-val-DAC[56] are two L-valyl ester prodrugs that are specific substrates of the intestinal transporter PEPT1 and enzyme BPHL. Data from PK studies in male Sprague−Dawley rats showed that valacyclovir[72] and L-val-DAC[56] both had significantly improved bioavailability over their parent nucleosides (46 vs 14% and 48.6 vs 27.86%, respectively). Once in the intestinal wall, a large portion of these L-valyl ester prodrugs are rapidly hydrolyzed by intestinal BPHL, and the remaining portion could be nearly completely hydrolyzed by hepatic BPHL, releasing the parent nucleosides to the circulation.[54,56] Unlike ProTides and cyclic phosphate prodrugs that are designed to bypass the first phosphorylation step, the L-valyl prodrug strategy is intended to improve bioavailability through

https://doi.org/10.1021/acsptsci.1c00016
ACS Pharmacol. Transl. Sci. 2021, 4, 870−887

enhancing intestinal uptake and leveraging rapid first-pass metabolism. Furthermore, since this type of prodrug can be efficiently delivered into intestinal cells by intestinal transporters and extensively hydrolyzed by intestinal BPHL, we envision that L-valyl ester prodrugs could be particularly effective in treating SARS-CoV-2 infection in the intestine.

Favipiravir, an antiviral nucleobase analog, was approved in Japan in 2014 for the treatment of influenza, and it has recently been granted emergency use authorization in Russia and Japan for COVID-19 treatment due to its potential against SARS-CoV-2.[42] An *in vitro* study showed that its active metabolite, T-705-RTP, is a potent inhibitor of the SARS-CoV-2 RdRp.[73] Another *in vitro* study showed that high concentrations of favipiravir could inhibit SARS-CoV-2 with an EC_{50} of 61.88 μM, suggesting a high dosage might be required for COVID-19 therapy.[74] In a phase III clinical trial, patients were treated with favipiravir tablets [3600 mg (1800 mg twice daily) (day 1) + 1600 mg (800 mg twice daily) (day 2 or later)] for up to a maximum of 14 days. The results showed significant benefits in terms of reduced recovery time, but adverse events were more frequent in the favipiravir arm than in the control arm (35.6 vs 8%).[75] In Japanese patients receiving favipiravir at a lower dose than the above phase III clinical trial, the frequency of adverse reactions was about 20%.[76] Hyperuricemia was the major adverse event, a consequence of renal transporter inhibition by favipiravir and its inactive metabolite T-705M1.[77] Two favipiravir inactivating enzymes, AO (major) and XO (minor),[78] are mainly expressed in the liver (Supplementary Figure 2), indicating that an extensive hepatic first-pass effect could exist. Moreover, considering that the intracellular activation of favipiravir requires both ribosylation and first phosphorylation, its activation may not be as efficient as that of ester prodrugs. To address these limitations, we designed two favipiravir prodrugs using the ProTide and L-valyl ester prodrug design strategies. We also applied the same strategies to design new prodrugs for GS-441524, the parent nucleoside of remdesivir. Molecular docking analysis revealed that compared with sofosbuvir the ProTide forms of favipiravir exhibited very similar binding energies for CTSA and CES1. Compared to sofosbuvir, the isopropyl ProTide form of GS-441524 may have higher CTSA binding affinity but lower CES1 binding affinity. The calculated binding energies of the proposed L-valyl ester prodrugs to PEPT1 and BPHL were generally comparable to those of valacyclovir. From a thermodynamic point of view, our docking results suggest that the ProTide and L-valyl ester prodrugs of favipiravir and GS-441524 have favorable binding affinities for target enzymes and transporters. Taken together, the metabolism and delivery features of ProTides and L-valyl ester prodrugs can be applicable to various nucleoside/nucleotide analogs with demonstrated *in vitro* anti-SARS-CoV-2 effects, such as favipiravir, ribavirin,[74] and β-*d*-N^4-hydroxycytidine (NHC; EIDD-1931).[71] Notably, whether the first phosphorylation is the rate-limiting step in the activation of GS-441524 and favipiravir in humans have not been fully established. Our proposed prodrugs with the ProTide and L-valyl-ester technology could offer two options: If the first phosphorylation is the rate-limiting step, then the ProTide form may be of help by bypassing the first phosphorylation. If not, then the L-valyl ester prodrug form could improve their oral availability. A recent study suggested that the second phosphorylation was the rate-limiting step in the activation of favipiravir in Madin–Darby canine kidney (MDCK) cells.[79] If this also occurs in SARS-CoV-2-infected cells, then the ProTide strategy may not be able to significantly improve its activation and efficacy, while the di- or triphosphate nucleoside/nucleotide prodrug design could be more favorable.[79] Thus, more work is needed to determine whether these proposed prodrugs for favipiravir and GS-441524 can boost their activations and anti-SARS-CoV-2 potency. The methods for synthesizing ProTide and L-valyl ester prodrugs can be seen in the previous studies.[44,80,81]

One potential limitation of this study is that the activating enzymes included in the analysis may not cover all enzymes involved in prodrug activation *in vivo*, leading to potential underestimation of the degree of activation in a tissue. However, the original studies for TAF and sofosbuvir screened more than 10 hydrolases when identifying the major activating enzymes,[37,38] and the enzymes responsible for hydrolysis of valacyclovir[36] and laninamivir octanoate[40] were identified by unbiased MS-based proteomics approaches, which had excellent coverage and throughput.

In summary, the expression patterns of serine hydrolases related to the activation and PK of anti-SARS-Cov-2 prodrugs vary significantly between different human tissues; thus, the activation rate of an antiviral prodrug can be tissue-dependent. The primary site for ester hydrolysis of ProTides is the liver, indicating that parenteral dosing should be considered when using these prodrugs to treat COVID-19. The L-valyl ester prodrug technology could be an effective approach for improving the bioavailability of oral nucleoside/nucleotide analogs, and probably offers the benefit of treating gastrointestinal viral infections. Moreover, a structure similar to that of laninamivir octanoate could be used as a reference for developing a long-acting inhaled anti-SARS-CoV-2 prodrug. Further investigations into different formulations and prodrug structures will lead to the development of a new generation of nucleoside or nucleotide prodrugs with improved efficacy and safety for COVID-19 treatment.

■ ASSOCIATED CONTENT

Supporting Information

The Supporting Information is available free of charge at https://pubs.acs.org/doi/10.1021/acsptsci.1c00016.

Demographic information on the tissue S9 fraction donors; gradient conditions of LC-MS/MS analysis; scaling the abundance and contribution of an enzyme in a tissue; concentrations of prodrugs and enzymes for the measurement of specific enzyme activity in previous studies; protein expression levels of serine hydrolases in the human lung, liver, intestine, and kidney; protein expression levels of HINT1 and HINT2 in in the human lung, liver, intestine, and kidney; putative metabolism pathway of favipiravir and the protein expression abundance of its deactivating enzymes. (PDF)

FASTA file of 238 human serine hydrolases (ZIP)

■ AUTHOR INFORMATION

Corresponding Author

Hao-Jie Zhu − *Department of Clinical Pharmacy, University of Michigan College of Pharmacy, Ann Arbor, Michigan 48109, United States;* orcid.org/0000-0002-2248-4419; Email: hjzhu@med.umich.edu

https://doi.org/10.1021/acsptsci.1c00016
ACS Pharmacol. Transl. Sci. 2021, 4, 870−887

Authors

Jiapeng Li − *Department of Clinical Pharmacy, University of Michigan College of Pharmacy, Ann Arbor, Michigan 48109, United States;* orcid.org/0000-0003-4321-1150

Shuhan Liu − *Department of Clinical Pharmacy, University of Michigan College of Pharmacy, Ann Arbor, Michigan 48109, United States; Department of Pharmaceutical Sciences, University of Pittsburgh School of Pharmacy, Pittsburgh, Pennsylvania 15261, United States;* orcid.org/0000-0002-6627-4843

Jian Shi − *Department of Clinical Pharmacy, University of Michigan College of Pharmacy, Ann Arbor, Michigan 48109, United States;* orcid.org/0000-0003-2609-0094

Xinwen Wang − *Department of Pharmaceutical Sciences, Northeast Ohio Medical University College of Pharmacy, Rootstown, Ohio 44272, United States;* orcid.org/0000-0001-8143-7017

Yanling Xue − *Department of Clinical Pharmacy, University of Michigan College of Pharmacy, Ann Arbor, Michigan 48109, United States*

Complete contact information is available at: https://pubs.acs.org/10.1021/acsptsci.1c00016

Author Contributions

H.Z. designed the prediction model. J.L, and H.Z. wrote the manuscript. J.L searched for, extracted, and analyzed data, and generated figures. S.L. conducted the molecular docking study. J.S. established the LC-MS/MS method for proteomics analysis. X.W. prepared the proteomics samples and run the LC-MS/MS analysis. X.W. and Y.X. analyzed the proteomics data. S.L., J.S., and X.W. edited and contributed to the manuscript. H.Z. obtained grant funding that supported this work.

Notes

The authors declare no competing financial interest.

■ ACKNOWLEDGMENTS

We thank Dr. Junmei Wang (University of Pittsburgh, School of Pharmacy) for supporting the molecular modeling analysis with Schrodinger software suite (Maestro version 11.2) in this study. This work was partially supported by the National Institutes of Health National Heart, Lung, and Blood Institute [R01 HL126969, H.Z.] and the Eunice Kennedy Shriver National Institute of Child Health and Human Development [R01 HD093612, J.S.M. and H.Z.].

■ REFERENCES

(1) Jawaid Akhtar, M. (2020) COVID19 inhibitors: A prospective therapeutics. *Bioorg. Chem. 101*, 104027.

(2) Elfiky, A. A. (2020) Ribavirin, Remdesivir, Sofosbuvir, Galidesivir, and Tenofovir against SARS-CoV-2 RNA dependent RNA polymerase (RdRp): A molecular docking study. *Life Sci. 253*, 117592.

(3) Zhu, W., Chen, C. Z., Gorshkov, K., Xu, M., Lo, D. C., and Zheng, W. (2020) RNA-Dependent RNA Polymerase as a Target for COVID-19 Drug Discovery. *SLAS Discovery 25*, 1141−1151.

(4) Chien, M., Anderson, T. K., Jockusch, S., Tao, C., Li, X., Kumar, S., Russo, J. J., Kirchdoerfer, R. N., and Ju, J. (2020) Nucleotide Analogues as Inhibitors of SARS-CoV-2 Polymerase, a Key Drug Target for COVID-19. *J. Proteome Res. 19*, 4690−4697.

(5) Pruijssers, A. J., George, A. S., Schäfer, A., Leist, S. R., Gralinksi, L. E., Dinnon, K. H., Yount, B. L., Agostini, M. L., Stevens, L. J., Chappell, J. D., Lu, X., Hughes, T. M., Gully, K., Martinez, D. R., Brown, A. J., Graham, R. L., Perry, J. K., Du Pont, V., Pitts, J., Ma, B., Babusis, D., Murakami, E., Feng, J. Y., Bilello, J. P., Porter, D. P., Cihlar, T., Baric, R. S., Denison, M. R., and Sheahan, T. P. (2020) Remdesivir Inhibits SARS-CoV-2 in Human Lung Cells and Chimeric SARS-CoV Expressing the SARS-CoV-2 RNA Polymerase in Mice. *Cell Rep. 32*, 107940.

(6) Williamson, B. N., Feldmann, F., Schwarz, B., Meade-White, K., Porter, D. P., Schulz, J., van Doremalen, N., Leighton, I., Yinda, C. K., Pérez-Pérez, L., Okumura, A., Lovaglio, J., Hanley, P. W., Saturday, G., Bosio, C. M., Anzick, S., Barbian, K., Cihlar, T., Martens, C., Scott, D. P., Munster, V. J., and de Wit, E. (2020) Clinical benefit of remdesivir in rhesus macaques infected with SARS-CoV-2. *Nature 585*, 273−276.

(7) Jockusch, S., Tao, C., Li, X., Chien, M., Kumar, S., Morozova, I., Kalachikov, S., Russo, J. J., and Ju, J. (2020) Sofosbuvir terminated RNA is more resistant to SARS-CoV-2 proofreader than RNA terminated by Remdesivir. *Sci. Rep. 10*, 16577.

(8) Spinner, C. D., Gottlieb, R. L., Criner, G. J., Arribas López, J. R., Cattelan, A. M., Soriano Viladomiu, A., Ogbuagu, O., Malhotra, P., Mullane, K. M., Castagna, A., et al. (2020) Effect of remdesivir vs standard care on clinical status at 11 days in patients with moderate COVID-19: a randomized clinical trial. *JAMA 324*, 1048−1057.

(9) Abbaspour Kasgari, H., Moradi, S., Shabani, A. M., Babamahmoodi, F., Davoudi Badabi, A. R., Davoudi, L., Alikhani, A., Hedayatizadeh Omran, A., Saeedi, M., Merat, S., Wentzel, H., Garratt, A., Levi, J., Simmons, B., Hill, A., and Tirgar Fakheri, H. (2020) Evaluation of the efficacy of sofosbuvir plus daclatasvir in combination with ribavirin for hospitalized COVID-19 patients with moderate disease compared with standard care: a single-centre, randomized controlled trial. *J. Antimicrob. Chemother. 75*, 3373−3378.

(10) Wang, Y., Zhang, D., Du, G., Du, R., Zhao, J., Jin, Y., Fu, S., Gao, L., Cheng, Z., Lu, Q., Hu, Y., Luo, G., Wang, K., Lu, Y., Li, H., Wang, S., Ruan, S., Yang, C., Mei, C., Wang, Y., Ding, D., Wu, F., Tang, X., Ye, X., Ye, Y., Liu, B., Yang, J., Yin, W., Wang, A., Fan, G., Zhou, F., Liu, Z., Gu, X., Xu, J., Shang, L., Zhang, Y., Cao, L., Guo, T., Wan, Y., Qin, H., Jiang, Y., Jaki, T., Hayden, F. G., Horby, P. W., Cao, B., and Wang, C. (2020) Remdesivir in adults with severe COVID-19: a randomised, double-blind, placebo-controlled, multicentre trial. *Lancet 395*, 1569−1578.

(11) Yan, V. C., and Muller, F. L. (2020) Advantages of the Parent Nucleoside GS-441524 over Remdesivir for Covid-19 Treatment. *ACS Med. Chem. Lett. 11*, 1361−1366.

(12) Sun, D. (2020) Remdesivir for Treatment of COVID-19: Combination of Pulmonary and IV Administration May Offer Aditional Benefit. *AAPS J. 22*, 77−77.

(13) De Schutter, C., Ehteshami, M., Hammond, E. T., Amblard, F., and Schinazi, R. F. (2018) Metabolism of Nucleosides and Nucleotides Prodrugs. *Curr. Pharm. Des. 23*, 6984−7002.

(14) Wiemer, A. J. (2020) Metabolic Efficacy of Phosphate Prodrugs and the Remdesivir Paradigm. *ACS Pharmacol. Transl. Sci. 3*, 613−626.

(15) Slusarczyk, M., Lopez, M. H., Balzarini, J., Mason, M., Jiang, W. G., Blagden, S., Thompson, E., Ghazaly, E., and McGuigan, C. (2014) Application of ProTide Technology to Gemcitabine: A Successful Approach to Overcome the Key Cancer Resistance Mechanisms Leads to a New Agent (NUC-1031) in Clinical Development. *J. Med. Chem. 57*, 1531−1542.

(16) Murakami, E., Wang, T., Park, Y., Hao, J., Lepist, E.-I., Babusis, D., and Ray, A. S. (2015) Implications of efficient hepatic delivery by tenofovir alafenamide (GS-7340) for hepatitis B virus therapy. *Antimicrob. Agents Chemother. 59*, 3563−3569.

(17) Simon, G. M., and Cravatt, B. F. (2010) Activity-based Proteomics of Enzyme Superfamilies: Serine Hydrolases as a Case Study. *J. Biol. Chem. 285*, 11051−11055.

(18) Long, J. Z., and Cravatt, B. F. (2011) The Metabolic Serine Hydrolases and Their Functions in Mammalian Physiology and Disease. *Chem. Rev. 111*, 6022−6063.

(19) Eastman, R. T., Roth, J. S., Brimacombe, K. R., Simeonov, A., Shen, M., Patnaik, S., and Hall, M. D. (2020) Remdesivir: A Review of Its Discovery and Development Leading to Emergency Use

Authorization for Treatment of COVID-19. *ACS Cent. Sci. 6*, 672−683.
(20) Mason, R. J. (2020) Pathogenesis of COVID-19 from a cell biology perspective. *Eur. Respir. J. 55*, 2000607.
(21) Tanner, J.-A., Prasad, B., Claw, K. G., Stapleton, P., Chaudhry, A., Schuetz, E. G., Thummel, K. E., and Tyndale, R. F. (2017) Predictors of Variation in CYP2A6 mRNA, Protein, and Enzyme Activity in a Human Liver Bank: Influence of Genetic and Nongenetic Factors. *J. Pharmacol. Exp. Ther. 360*, 129−139.
(22) Dostalek, M., Court, M. H., Yan, B., and Akhlaghi, F. (2011) Significantly reduced cytochrome P450 3A4 expression and activity in liver from humans with diabetes mellitus. *Br. J. Pharmacol. 163*, 937−947.
(23) Ohtsuki, S., Schaefer, O., Kawakami, H., Inoue, T., Liehner, S., Saito, A., Ishiguro, N., Kishimoto, W., Ludwig-Schwellinger, E., Ebner, T., and Terasaki, T. (2012) Simultaneous Absolute Protein Quantification of Transporters, Cytochromes P450, and UDP-Glucuronosyltransferases as a Novel Approach for the Characterization of Individual Human Liver: Comparison with mRNA Levels and Activities. *Drug Metab. Dispos. 40*, 83−92.
(24) Basit, A., Neradugomma, N. K., Wolford, C., Fan, P. W., Murray, B., Takahashi, R. H., Khojasteh, S. C., Smith, B. J., Heyward, S., Totah, R. A., Kelly, E. J., and Prasad, B. (2020) Characterization of Differential Tissue Abundance of Major Non-CYP Enzymes in Human. *Mol. Pharmaceutics 17*, 4114−4124.
(25) He, B., Shi, J., Wang, X., Jiang, H., and Zhu, H.-J. (2019) Label-free absolute protein quantification with data-independent acquisition. *J. Proteomics 200*, 51−59.
(26) Shi, J., Wang, X., Lyu, L., Jiang, H., and Zhu, H.-J. (2018) Comparison of protein expression between human livers and the hepatic cell lines HepG2, Hep3B, and Huh7 using SWATH and MRM-HR proteomics: Focusing on drug-metabolizing enzymes. *Drug Metab. Pharmacokinet. 33*, 133−140.
(27) Alanazi, A. S., James, E., and Mehellou, Y. (2019) The ProTide Prodrug Technology: Where Next? *ACS Med. Chem. Lett. 10*, 2−5.
(28) Mackman, R. L., Ray, A. S., Hui, H. C., Zhang, L., Birkus, G., Boojamra, C. G., Desai, M. C., Douglas, J. L., Gao, Y., Grant, D., Laflamme, G., Lin, K.-Y., Markevitch, D. Y., Mishra, R., McDermott, M., Pakdaman, R., Petrakovsky, O. V., Vela, J. E., and Cihlar, T. (2010) Discovery of GS-9131: Design, synthesis and optimization of amidate prodrugs of the novel nucleoside phosphonate HIV reverse transcriptase (RT) inhibitor GS-9148. *Bioorg. Med. Chem. 18*, 3606−3617.
(29) Furman, P. A., Murakami, E., Niu, C., Lam, A. M., Espiritu, C., Bansal, S., Bao, H., Tolstykh, T., Micolochick Steuer, H., Keilman, M., Zennou, V., Bourne, N., Veselenak, R. L., Chang, W., Ross, B. S., Du, J., Otto, M. J., and Sofia, M. J. (2011) Activity and the metabolic activation pathway of the potent and selective hepatitis C virus pronucleotide inhibitor PSI-353661. *Antiviral Res. 91*, 120−132.
(30) Ishizuka, H., Toyama, K., Yoshiba, S., Okabe, H., and Furuie, H. (2012) Intrapulmonary distribution and pharmacokinetics of laninamivir, a neuraminidase inhibitor, after a single inhaled administration of its prodrug, laninamivir octanoate, in healthy volunteers. *Antimicrob. Agents Chemother. 56*, 3873−3878.
(31) Feng, J. Y., Wang, T., Park, Y., Babusis, D., Birkus, G., Xu, Y., Voitenleitner, C., Fenaux, M., Yang, H., and Eng, S. (2018) Nucleotide prodrug containing a nonproteinogenic amino acid to improve oral delivery of a hepatitis C virus treatment. *Antimicrob. Agents Chemother. 62*, e00620-18.
(32) Niu, C., Tolstykh, T., Bao, H., Park, Y., Babusis, D., Lam, A. M., Bansal, S., Du, J., Chang, W., Reddy, P. G., et al. (2012) Metabolic activation of the anti-hepatitis C virus nucleotide prodrug PSI-352938. *Antimicrob. Agents Chemother. 56*, 3767−3775.
(33) Jonckers, T. H. M., Tahri, A., Vijgen, L., Berke, J. M., Lachau-Durand, S., Stoops, B., Snoeys, J., Leclercq, L., Tambuyzer, L., Lin, T.-I., Simmen, K., and Raboisson, P. (2016) Discovery of 1-((2R,4aR,6R,7R,7aR)-2-Isopropoxy-2-oxidodihydro-4H,6H-spiro-[furo[3,2-d][1,3,2]dioxaphosphinine-7,2′-oxetan]-6-yl)pyrimidine-2,4(1H,3H)-dione (JNJ-54257099), a 3′-5′-Cyclic Phosphate Ester Prodrug of 2′-Deoxy-2′-Spirooxetane Uridine Triphosphate Useful for HCV Inhibition. *J. Med. Chem. 59*, 5790−5798.
(34) Tao, W., Zhao, D., Sun, M., Li, M., Zhang, X., He, Z., Sun, Y., and Sun, J. (2017) Enzymatic activation of double-targeted 5′-O-l-valyl-decitabine prodrug by biphenyl hydrolase-like protein and its molecular design basis. *Drug Delivery Transl. Res. 7*, 304−311.
(35) Kim, I., Song, X., Vig, B. S., Mittal, S., Shin, H.-C., Lorenzi, P. J., and Amidon, G. L. (2004) A Novel Nucleoside Prodrug-Activating Enzyme: Substrate Specificity of Biphenyl Hydrolase-like Protein. *Mol. Pharmaceutics 1*, 117−127.
(36) Shenoy, V. M., Thompson, B. R., Shi, J., Zhu, H.-J., Smith, D. E., and Amidon, G. L. (2020) Chemoproteomic Identification of Serine Hydrolase RBBP9 as a Valacyclovir-Activating Enzyme. *Mol. Pharmaceutics 17*, 1706−1714.
(37) Birkus, G., Kutty, N., He, G.-X., Mulato, A., Lee, W., McDermott, M., and Cihlar, T. (2008) Activation of 9-[(R)-2-[[(S)-[[(S)-1-(Isopropoxycarbonyl) ethyl] amino] phenoxyphosphinyl]-methoxy] propyl] adenine (GS-7340) and other tenofovir phosphonoamidate prodrugs by human proteases. *Mol. Pharmacol. 74*, 92−100.
(38) Murakami, E., Tolstykh, T., Bao, H., Niu, C., Steuer, H. M. M., Bao, D., Chang, W., Espiritu, C., Bansal, S., Lam, A. M., et al. (2010) Mechanism of activation of PSI-7851 and its diastereoisomer PSI-7977. *J. Biol. Chem. 285*, 34337−34347.
(39) Murakami, E., Wang, T., Babusis, D., Lepist, E.-I., Sauer, D., Park, Y., Vela, J. E., Shih, R., Birkus, G., Stefanidis, D., Kim, C. U., Cho, A., and Ray, A. S. (2014) Metabolism and Pharmacokinetics of the Anti-Hepatitis C Virus Nucleotide Prodrug GS-6620. *Antimicrob. Agents Chemother. 58*, 1943−1951.
(40) Koyama, K., Ogura, Y., Nakai, D., Watanabe, M., Munemasa, T., Oofune, Y., Kubota, K., Shinagawa, A., and Izumi, T. (2014) Identification of Bioactivating Enzymes Involved in the Hydrolysis of Laninamivir Octanoate, a Long-Acting Neuraminidase Inhibitor, in Human Pulmonary Tissue. *Drug Metab. Dispos. 42*, 1031−1038.
(41) Du, Y.-X., and Chen, X.-P. (2020) Favipiravir: Pharmacokinetics and Concerns About Clinical Trials for 2019-nCoV Infection. *Clin. Pharmacol. Ther. 108*, 242−247.
(42) Agrawal, U., Raju, R., and Udwadia, Z. F. (2020) Favipiravir: A new and emerging antiviral option in COVID-19. *Med. J. Armed Forces India. 76*, 370−376.
(43) Eloy, P., Solas, C., Touret, F., Mentré, F., Malvy, D., de Lamballerie, X., and Guedj, J. (2020) Dose Rationale for Favipiravir Use in Patients Infected With SARS-CoV-2. *Clin. Pharmacol. Ther. 108*, 188−188.
(44) Siegel, D., Hui, H. C., Doerffler, E., Clarke, M. O., Chun, K., Zhang, L., Neville, S., Carra, E., Lew, W., Ross, B., Wang, Q., Wolfe, L., Jordan, R., Soloveva, V., Knox, J., Perry, J., Perron, M., Stray, K. M., Barauskas, O., Feng, J. Y., Xu, Y., Lee, G., Rheingold, A. L., Ray, A. S., Bannister, R., Strickley, R., Swaminathan, S., Lee, W. A., Bavari, S., Cihlar, T., Lo, M. K., Warren, T. K., and Mackman, R. L. (2017) Discovery and Synthesis of a Phosphoramidate Prodrug of a Pyrrolo([2,1-f][triazin-4-amino] Adenine C-Nucleoside (GS-5734) for the Treatment of Ebola and Emerging Viruses. *J. Med. Chem. 60*, 1648−1661.
(45) Humeniuk, R., Mathias, A., Cao, H., Osinusi, A., Shen, G., Chng, E., Ling, J., Vu, A., and German, P. (2020) Safety, Tolerability, and Pharmacokinetics of Remdesivir, An Antiviral for Treatment of COVID-19, in Healthy Subjects. *Clin. Transl. Sci. 13*, 896−906.
(46) Friesner, R. A., Banks, J. L., Murphy, R. B., Halgren, T. A., Klicic, J. J., Mainz, D. T., Repasky, M. P., Knoll, E. H., Shelley, M., Perry, J. K., Shaw, D. E., Francis, P., and Shenkin, P. S. (2004) Glide: A New Approach for Rapid, Accurate Docking and Scoring. 1. Method and Assessment of Docking Accuracy. *J. Med. Chem. 47*, 1739−1749.
(47) Birkus, G., Wang, R., Liu, X., Kutty, N., MacArthur, H., Cihlar, T., Gibbs, C., Swaminathan, S., Lee, W., and McDermott, M. (2007) Cathepsin A is the major hydrolase catalyzing the intracellular hydrolysis of the antiretroviral nucleotide phosphonoamidate

https://doi.org/10.1021/acsptsci.1c00016
ACS Pharmacol. Transl. Sci. 2021, 4, 870−887

prodrugs GS-7340 and GS-9131. *Antimicrob. Agents Chemother. 51*, 543−550.
(48) Babusis, D., Phan, T. K., Lee, W. A., Watkins, W. J., and Ray, A. S. (2013) Mechanism for effective lymphoid cell and tissue loading following oral administration of nucleotide prodrug GS-7340. *Mol. Pharmaceutics 10*, 459−466.
(49) Sofia, M. J., Bao, D., Chang, W., Du, J., Nagarathnam, D., Rachakonda, S., Reddy, P. G., Ross, B. S., Wang, P., Zhang, H.-R., et al. (2010) Discovery of a β-d-2′-deoxy-2′-α-fluoro-2′-β-C-methyluridine nucleotide prodrug (PSI-7977) for the treatment of hepatitis C virus. *J. Med. Chem. 53*, 7202−7218.
(50) Chang, W., Bao, D., Chun, B.-K., Naduthambi, D., Nagarathnam, D., Rachakonda, S., Reddy, P. G., Ross, B. S., Zhang, H.-R., Bansal, S., Espiritu, C. L., Keilman, M., Lam, A. M., Niu, C., Steuer, H. M., Furman, P. A., Otto, M. J., and Sofia, M. J. (2011) Discovery of PSI-353661, a Novel Purine Nucleotide Prodrug for the Treatment of HCV Infection. *ACS Med. Chem. Lett. 2*, 130−135.
(51) Landowski, C. P., Sun, D., Foster, D. R., Menon, S. S., Barnett, J. L., Welage, L. S., Ramachandran, C., and Amidon, G. L. (2003) Gene Expression in the Human Intestine and Correlation with Oral Valacyclovir Pharmacokinetic Parameters. *J. Pharmacol. Exp. Ther. 306*, 778−786.
(52) Balimane, P. V., Tamai, I., Guo, A., Nakanishi, T., Kitada, H., Leibach, F. H., Tsuji, A., and Sinko, P. J. (1998) Direct evidence for peptide transporter (PepT1)-mediated uptake of a nonpeptide prodrug, valacyclovir. *Biochem. Biophys. Res. Commun. 250*, 246−251.
(53) Yang, B., Hu, Y., and Smith, D. E. (2013) Impact of peptide transporter 1 on the intestinal absorption and pharmacokinetics of valacyclovir after oral dose escalation in wild-type and PepT1 knockout mice. *Drug Metab. Dispos. 41*, 1867−1874.
(54) MacDougall, C., and Guglielmo, B. J. (2004) Pharmacokinetics of valaciclovir. *J. Antimicrob. Chemother. 53*, 899−901.
(55) Lai, L., Xu, Z., Zhou, J., Lee, K.-D., and Amidon, G. L. (2008) Molecular Basis of Prodrug Activation by Human Valacyclovirase, an α-Amino Acid Ester Hydrolase. *J. Biol. Chem. 283*, 9318−9327.
(56) Tao, W., Zhao, D., Sun, M., Wang, Z., Lin, B., Bao, Y., Li, Y., He, Z., Sun, Y., and Sun, J. (2018) Intestinal absorption and activation of decitabine amino acid ester prodrugs mediated by peptide transporter PEPT1 and enterocyte enzymes. *Int. J. Pharm. 541*, 64−71.
(57) Bencharit, S., Morton, C. L., Xue, Y., Potter, P. M., and Redinbo, M. R. (2003) Structural basis of heroin and cocaine metabolism by a promiscuous human drug-processing enzyme. *Nat. Struct. Mol. Biol. 10*, 349−356.
(58) Schreuder, H. A., Liesum, A., Kroll, K., Böhnisch, B., Buning, C., Ruf, S., and Sadowski, T. (2014) Crystal structure of cathepsin A, a novel target for the treatment of cardiovascular diseases. *Biochem. Biophys. Res. Commun. 445*, 451−456.
(59) Schaefer, I.-M., Padera, R. F., Solomon, I. H., Kanjilal, S., Hammer, M. M., Hornick, J. L., and Sholl, L. M. (2020) In situ detection of SARS-CoV-2 in lungs and airways of patients with COVID-19. *Mod. Pathol. 33*, 2104−2114.
(60) Crapo, J. D., Barry, B. E., Gehr, P., Bachofen, M., and Weibel, E. R. (1982) Cell Number and Cell Characteristics of the Normal Human Lung. *Am. Rev. Respir. Dis. 126*, 332−337.
(61) Roozbeh, F., Saeedi, M., Alizadeh-Navaei, R., Hedayatizadeh-Omran, A., Merat, S., Wentzel, H., Levi, J., Hill, A., and Shamshirian, A. (2021) Sofosbuvir and daclatasvir for the treatment of COVID-19 outpatients: a double-blind, randomized controlled trial. *J. Antimicrob. Chemother. 76*, 753−757.
(62) Van Rompay, A. R., Johansson, M., and Karlsson, A. (2000) Phosphorylation of nucleosides and nucleoside analogs by mammalian nucleoside monophosphate kinases. *Pharmacol. Ther. 87*, 189−198.
(63) Shah, R., Maize, K. M., Zhou, X., Finzel, B. C., and Wagner, C. R. (2017) Caught before Released: Structural Mapping of the Reaction Trajectory for the Sofosbuvir Activating Enzyme, Human Histidine Triad Nucleotide Binding Protein 1 (hHint1). *Biochemistry 56*, 3559−3570.
(64) Chou, T.-F., Baraniak, J., Kaczmarek, R., Zhou, X., Cheng, J., Ghosh, B., and Wagner, C. R. (2007) Phosphoramidate Pronucleotides: A Comparison of the Phosphoramidase Substrate Specificity of Human and Escherichia coli Histidine Triad Nucleotide Binding Proteins. *Mol. Pharmaceutics 4*, 208−217.
(65) Birkus, G., Kutty, N., Frey, C. R., Shribata, R., Chou, T., Wagner, C., McDermott, M., and Cihlar, T. (2011) Role of Cathepsin A and Lysosomes in the Intracellular Activation of Novel Antipapillomavirus Agent GS-9191. *Antimicrob. Agents Chemother. 55*, 2166−2173.
(66) Li, Y., Cao, L., Li, G., Cong, F., Li, Y., Sun, J., Luo, Y., Chen, G., Li, G., and Wang, P. et al. (2021) Remdesivir Metabolite GS-441524 Effectively Inhibits SARS-CoV-2 Infection in Mouse Models. *J. Med. Chem.* DOI: 10.1021/acs.jmedchem.0c01929.
(67) Sahakijpijarn, S., Moon, C., Koleng, J. J., Christensen, D. J., and Williams, R. O. (2020) Development of Remdesivir as a Dry Powder for Inhalation by Thin Film Freezing. *Pharmaceutics 12*, 1002.
(68) Kashiwagi, S., Yoshida, S., Yamaguchi, H., Niwa, S., Mitsui, N., Tanigawa, M., Shiosakai, K., Yamanouchi, N., Shiozawa, T., and Yamaguchi, F. (2012) Safety of the long-acting neuraminidase inhibitor laninamivir octanoate hydrate in post-marketing surveillance. *Int. J. Antimicrob. Agents 40*, 381−388.
(69) Watanabe, A., Chang, S.-C., Kim, M. J., Chu, D. W., and Ohashi, Y. (2010) Long-Acting Neuraminidase Inhibitor Laninamivir Octanoate versus Oseltamivir for Treatment of Influenza: A Double-Blind, Randomized, Noninferiority Clinical Trial. *Clin. Infect. Dis. 51*, 1167−1175.
(70) Stanifer, M. L., Kee, C., Cortese, M., Zumaran, C. M., Triana, S., Mukenhirn, M., Kraeusslich, H.-G., Alexandrov, T., Bartenschlager, R., and Boulant, S. (2020) Critical Role of Type III Interferon in Controlling SARS-CoV-2 Infection in Human Intestinal Epithelial Cells. *Cell Rep. 32*, 107863.
(71) Sheahan, T. P., Sims, A. C., Zhou, S., Graham, R. L., Pruijssers, A. J., Agostini, M. L., Leist, S. R., Schäfer, A., Dinnon, K. H., Stevens, L. J., Chappell, J. D., Lu, X., Hughes, T. M., George, A. S., Hill, C. S., Montgomery, S. A., Brown, A. J., Bluemling, G. R., Natchus, M. G., Saindane, M., Kolykhalov, A. A., Painter, G., Harcourt, J., Tamin, A., Thornburg, N. J., Swanstrom, R., Denison, M. R., and Baric, R. S. (2020) An orally bioavailable broad-spectrum antiviral inhibits SARS-CoV-2 in human airway epithelial cell cultures and multiple coronaviruses in mice. *Sci. Transl. Med. 12*, eabb5883.
(72) Thomsen, A. E., Christensen, M. S., Bagger, M. A., and Steffansen, B. (2004) Acyclovir prodrug for the intestinal di/tripeptide transporter PEPT1: comparison of in vivo bioavailability in rats and transport in Caco-2 cells. *Eur. J. Pharm. Sci. 23*, 319−325.
(73) Shannon, A., Selisko, B., Le, N.-T.-T., Huchting, J., Touret, F., Piorkowski, G., Fattorini, V., Ferron, F., Decroly, E., Meier, C., et al. (2020) Rapid incorporation of Favipiravir by the fast and permissive viral RNA polymerase complex results in SARS-CoV-2 lethal mutagenesis. *Nat. Commun. 11*, 4682.
(74) Wang, M., Cao, R., Zhang, L., Yang, X., Liu, J., Xu, M., Shi, Z., Hu, Z., Zhong, W., and Xiao, G. (2020) Remdesivir and chloroquine effectively inhibit the recently emerged novel coronavirus (2019-nCoV) in vitro. *Cell Res. 30*, 269−271.
(75) Udwadia, Z. F., Singh, P., Barkate, H., Patil, S., Rangwala, S., Pendse, A., Kadam, J., Wu, W., Caracta, C. F., and Tandon, M. (2021) Efficacy and safety of favipiravir, an oral RNA-dependent RNA polymerase inhibitor, in mild-to-moderate COVID-19: A randomized, comparative, open-label, multicenter, phase 3 clinical trial. *Int. J. Infect. Dis. 103*, 62−71.
(76) The Japanese Association for Infectious Diseases, Favipiravir Observational Study Group. (May 15, 2020) Preliminary Report of the Favipiravir Observational Study in Japan. Japan release date: May 26, 2020. https://www.kansensho.or.jp/uploads/files/topics/2019ncov/covid19_casereport_en_200529.pdf (Accessed on Oct. 22, 2020).
(77) Mishima, E., Anzai, N., Miyazaki, M., and Abe, T. (2020) Uric Acid Elevation by Favipiravir, an Antiviral Drug. *Tohoku J. Exp. Med. 251*, 87−90.

(78) Pharmaceuticals and Medical Devices Agency, Ministry of Health, Labor, and Welfare, Government of Japan. (January 23, 2014) Review Report. https://www.pmda.go.jp/files/000210319.pdf, pp 33−39 (Accessed on Oct. 22, 2020).
(79) Huchting, J., Vanderlinden, E., Winkler, M., Nasser, H., Naesens, L., and Meier, C. (2018) Prodrugs of the Phosphoribosylated Forms of Hydroxypyrazinecarboxamide Pseudobase T-705 and Its De-Fluoro Analogue T-1105 as Potent Influenza Virus Inhibitors. *J. Med. Chem. 61*, 6193−6210.
(80) Wang, G., Wan, J., Hu, Y., Wu, X., Prhavc, M., Dyatkina, N., Rajwanshi, V. K., Smith, D. B., Jekle, A., Kinkade, A., Symons, J. A., Jin, Z., Deval, J., Zhang, Q., Tam, Y., Chanda, S., Blatt, L., and Beigelman, L. (2016) Synthesis and Anti-Influenza Activity of Pyridine, Pyridazine, and Pyrimidine C-Nucleosides as Favipiravir (T-705) Analogues. *J. Med. Chem. 59*, 4611−4624.
(81) Zhang, Y., Sun, J., Gao, Y., Jin, L., Xu, Y., Lian, H., Sun, Y., Sun, Y., Liu, J., Fan, R., Zhang, T., and He, Z. (2013) A Carrier-Mediated Prodrug Approach To Improve the Oral Absorption of Antileukemic Drug Decitabine. *Mol. Pharmaceutics 10*, 3195−3202.

https://doi.org/10.1021/acsptsci.1c00016
ACS Pharmacol. Transl. Sci. 2021, 4, 870−887